Article

TTF1 suppresses neuroblastoma growth and induces neuroblastoma differentiation by targeting TrkA and the miR-204/TrkB axis

Tianyou Yang,
Jiahao Li, Zhenjian
Zhuo, ..., Yan Zou,
Jing He, Huimin
Xia

monknut@126.com (Y.Z.)
hejing198374@gmail.com
(J.H.)
xia-huimin@foxmail.com (H.X.)

Highlights

TTF1, TrkA, and miR-204
were lowly expressed in
undifferentiated NB
tissues

TTF1 promoter was
hypermethylated in
undifferentiated NB
tissues and cells

TTF1 suppressed
proliferation of NB cells by
regulating TrkA and the
miR-204-TrkB axis

TTF1 suppressed tumor
growth and promoted
neurogenic differentiation
in vivo

iScience

Article

TTF1 suppresses neuroblastoma growth and induces neuroblastoma differentiation by targeting TrkA and the miR-204/TrkB axis

Tianyou Yang,[1,2] Jiahao Li,[2] Zhenjian Zhuo,[2] Huijuan Zeng,[2] Tianbao Tan,[2] Lei Miao,[2] Manna Zheng,[2] Jiliang Yang,[2] Jing Pan,[2] Chao Hu,[2] Yan Zou,[2,*] Jing He,[2,*] and Huimin Xia[1,2,3,*]

SUMMARY

Neuroblastoma (NB) is the most common extracranial malignant solid tumor in children. We found that TTF1, TrkA, and miR-204 were lowly expressed, whereas TrkB was highly expressed in undifferentiated NB tissues. Meanwhile, TTF1 expression correlated positively with TrkA and miR-204 expression but negatively with TrkB expression. The *TTF1* promoter was hypermethylated in undifferentiated NB tissues and SK-N-BE cells, leading to *TTF1* downregulation. We also identified miR-204, which directly targets TrkB, as a transcriptional target of TTF1. Functionally, TTF1 suppressed proliferation, migration, and invasion of NB cells, whereas induced cell cycle arrest, apoptosis, and autophagy of NB cells by regulating TrkA and the miR-204-TrkB axis. Furthermore, TTF1 suppressed tumor growth and promoted neurogenic differentiation in a NB xenograft mouse model. Our study demonstrates that TTF1 reduces tumor growth and induces neurogenic differentiation in NB by directly targeting TrkA and the miR-204/TrkB axis.

INTRODUCTION

Neuroblastoma (NB) is the most common extracranial solid malignancy in children, accounting for approximately 15% of all deaths caused by pediatric cancer (Brodeur, 2003). NB has heterogeneous clinical characteristics and outcomes, ranging from spontaneous regression to aggressive progression and distant metastasis (Ackermann et al., 2018; Maris et al., 2007). Although the majority of patients with low and intermediate-risk NB can currently be cured with minimal treatment, over half of all patients with high-risk NB experienced progression or relapse despite receiving intensified treatment regimen and immunotherapy. Consequently, the overall five-year survival rate for patients with high-risk NB is around 50% (London et al., 2011; Park et al., 2013). Dysregulated neuronal differentiation is considered to be a critical regulator of NB initiation and progression (Brodeur, 2018). Indeed, studies have demonstrated that stage IV-S NB can spontaneously regress and that well-differentiated NB can differentiate into benign ganglioneuroma (GN) (Mohlin et al., 2011; Newman and Nuchtern, 2016). However, the mechanism underlying spontaneous regression and NB differentiation remains largely unknown. An improved understanding of this mechanism could provide better targets for treating NB and thereby improve the outcome of patients with NB.

Evidence suggests that the receptor tyrosine kinase (Trk) family of neurotrophin receptors are critically involved in the regulation of neuronal development and also play a critical role in the regulation of differentiation, proliferation, and invasion of NB (Stasevych et al., 2015; Thomaz et al., 2020). The three types of Trk, TrkA, TrkB, and TrkC (Fung et al., 2011), exert distinct roles in the pathogenesis of NB with their respective ligands: nerve growth factor (NGF), brain-derived neurotrophic factor (BDNF), and neurotrophin-3 (NT-3) (Brodeur et al., 2014). Previous studies have shown that TrkA expression is significantly lower in advanced NB and is inversely associated with MYCN amplification (Kogner et al., 1993; Nakagawara et al., 1992), whereas elevated TrkA expression has been reported in patients with spontaneously-regressed stage IV-S NB and well-differentiated NB (Thress et al., 2009). Similarly, high TrkC level correlates negatively with MYCN amplification in NB as well as a favourable outcome (Ryden et al., 1996; Yamashiro et al., 1997). Conversely, TrkB overexpression has been reported in more than 50% of patients with high-risk NB and is associated with aggressive progression and an unfavourable outcome

[1]The Second School of Clinical Medicine, Southern Medical University, Guangzhou 510280, China

[2]Department of Pediatric Surgery, Guangzhou Women and Children's Medical Center, Guangzhou Medical University, Guangzhou 510623, China

[3]Lead contact

*Correspondence:
monknut@126.com (Y.Z.),
hejing198374@gmail.com (J.H.),
xia-huimin@foxmail.com (H.X.)
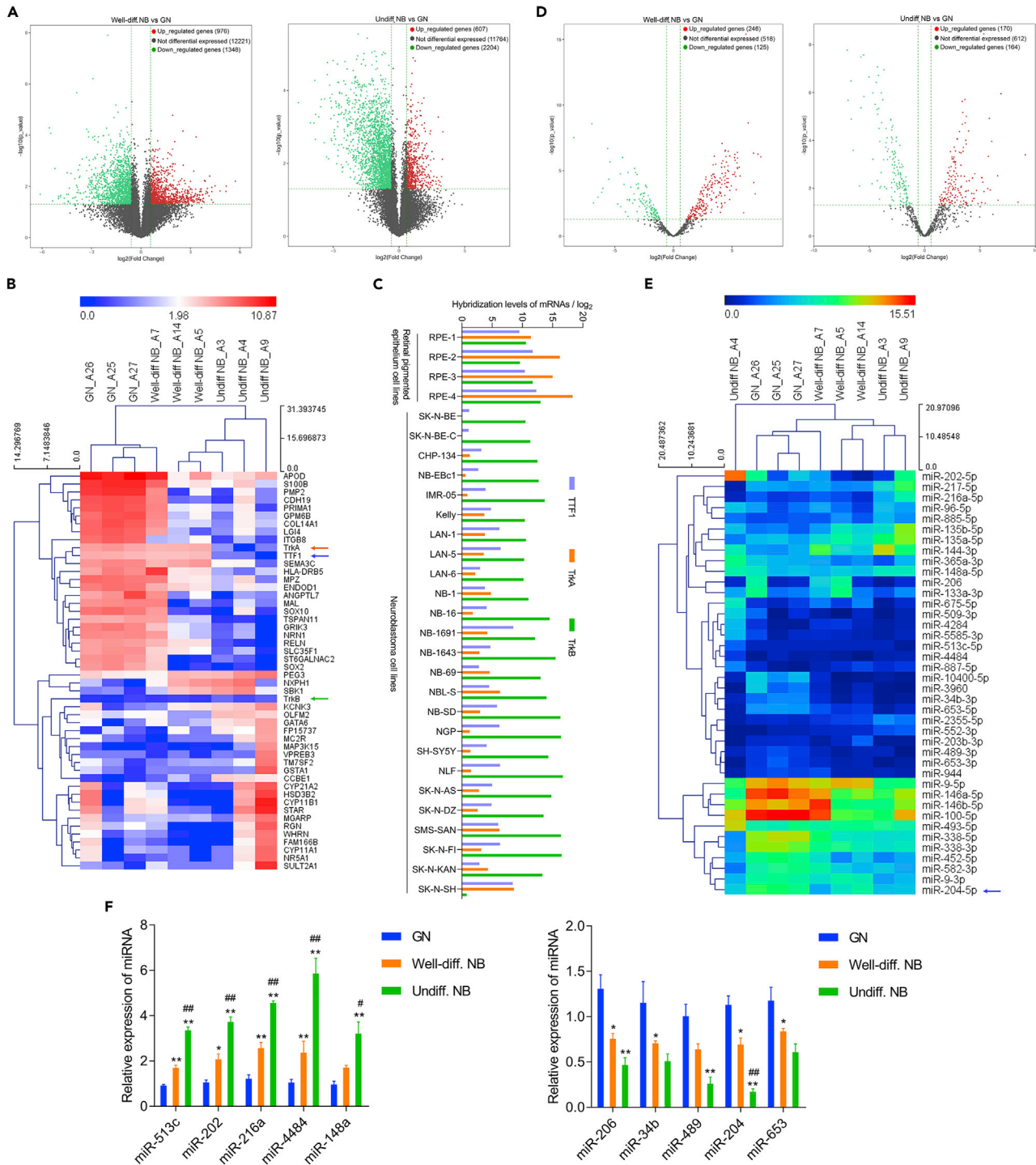
Figure 1. Screening and identification of DEGs and DEMs in NB progression

(A)Volcano plot of DEGs (>2-fold regulation, false discovery rate <0.05) in GN, well-differentiated, and undifferentiated NB tissues identified using RNA-seq.

(B) Cluster thermogram of DEGs.

(C) TTF1, TrkA, and TrkB expressions in NB cell line from a GEO database (GSE78061).

(D)Volcano plot of DEMs between GN and undifferentiated NB or well-differentiated NB. Vertical lines correspond to 2-fold upregulation and downre-gulation, respectively. The horizontal line represents p = 0.05.

Figure 1. Continued

(E) Heat map of 40 differently expressed miRNAs in the above three groups. Red indicates high miRNA expression. Green indicates low miRNA expression.
(F) The expression of five down- and five up-regulated miRNAs were verified by RT-qPCR analysis. Data are represented as mean ± SD. *p < 0.05, **p < 0.01 vs. GN; #p < 0.05, ##p < 0.01 vs. well-differentiated NB.

(Nakagawara et al., 1994). In NB cell lines, the BDNF/TrkB axis has also been shown to induce angiogenesis and maintain an undifferentiated phenotype, whereas the NGF/TrkA axis can promote NB cell differentiation (Khotskaya et al., 2017; Pacenta and Macy, 2018). MicroRNAs (miRNAs) are post-transcriptional regulators of 18–22 nucleotides in length that suppress the translation of specific target mRNAs by binding to their 3′UTRs (Bartel, 2004). Abnormal expression of miRNAs is also considered to be closely related to the initiation, differentiation, and development of NB (Aravindan et al., 2019; Maugeri et al., 2016). For instance, Leleesha et al. (Samaraweera et al., 2014) found that exogenous miR-124 overexpression promoted the terminal differentiation of NB cells and inhibited their tumorigenicity. Similarly, Fontana et al. (2008) found that miR-17-5p cluster expression correlated positively with MYCN amplification in NB cell lines, and enhanced NB cell proliferation. MiR-34 is an important tumor suppressor that can inhibit NB cell growth by negatively regulating MYCN, E2F3, and other genes related to cell proliferation and apoptosis (Stallings, 2009).

In this study, a high-throughput RNA sequencing (RNA-seq) technology was used to identify differentially expressed genes (DEGs) and miRNAs (DEMs) in ganglioneuroma (GN), well-differentiated NB, and undifferentiated NB tissue, and to identify key regulators of NB differentiation. We found that TrkA, TrkB, and thyroid transcription factor 1 (TTF1) could be molecular markers that exert important roles in NB differentiation. The deletion of TTF1, a critical transcriptional regulator of thyroid development and differentiation by directly up-regulating thyroglobulin and thyroid-specific genes (Guazzi et al., 1990), has been associated with the occurrence of thyroid cancer (Espinoza et al., 2001). TTF1 knockdown also inhibited the differentiation of lung adenocarcinoma cells and enhanced their colonization and distant metastasis in a mouse model of lung adenocarcinoma mediated by K-Ras and p53 double mutations (Winslow et al., 2011). In addition, decreased TTF1 expression may indicate a poor prognosis in patients with gastric cancer (Zhao et al., 2014). We here demonstrated that low expression of TTF1 owing to promoter hypermethylation which led to up-regulation of TrkA and down-regulation of TrkB via its transitional target miR-204 was the crucial step of the development and undifferentiation of NB.

RESULTS

Screening and identification of DEGs and DEMs involved in NB progression

First, we investigated the gene and miRNA expression profiles of GN (n = 3), well-differentiated NB (n = 3), and undifferentiated NB (n = 3) tissues using RNA-seq. Patients' age ranged from 0 month to 8 years, with a median age of 10 months. The distribution of gene expressions was displayed as a volcano plot (Figure 1A) and DEGs with a fold change of >2 and a false discovery rate of <0.05 were selected for GO functional and KEGG pathway enrichment analyses. Enriched GO functions (p < 0.01) for the downregulated (Figure S1A) and upregulated (Figure S1B) target genes were identified, including MF, BP, and CC. KEGG pathway analysis indicated that the target downregulated genes were mainly enriched in the PI3K-Akt and P53 signaling pathways (Figure S1C), while the target upregulated genes were enriched in the Foxo signaling pathway and cancer-related pathways (Figure S1D). Based on the RNA-seq results, we displayed the DEGs using a cluster thermogram and found that TTF1/NKX2.1 was dysregulated in tumor differentiation. Compared to GN tissues, TTF1 and TrkA were downregulated in undifferentiated NB, whereas TrkB expression did not differ among these groups (Figure 1B). Gene expression analysis of a public GEO database (GSE78061) including 25 NB cells confirmed that TTF1 and TrkA mRNA levels were significantly lower in NB cell lines than in 4 retinal pigmented epithelium (RPE) cell lines, whereas TrkB mRNA levels did not differ (Figure 1C). DEMs with a fold change of >2 and an FDR of <0.05 were selected and showed in a volcano plot (Figure 1D), whereas the expression of 40 DEMs in GN, undifferentiated NB, and well-differentiated NB tissues were displayed in a clustered heatmap (Figure 1E). The expression of the top five up- and down-regulated miRNAs was verified by RT-qPCR. As expected, miR-206, miR-34b, miR-489, miR-204, and miR-653 were significantly downregulated in well-differentiated and undifferentiated NB compared to GN, whereas miR-513c, miR-203, miR-216a, miR-4484, and miR-148a were significantly upregulated (Figure 1F). Notably, the expression of these five upregulated miRNAs was clearly elevated in undifferentiated NB compared to well-differentiated NB. Considering the potential role of miR-204 in glioma stem-like cell differentiation (Ying et al., 2013), we selected miR-204 for further experiments.
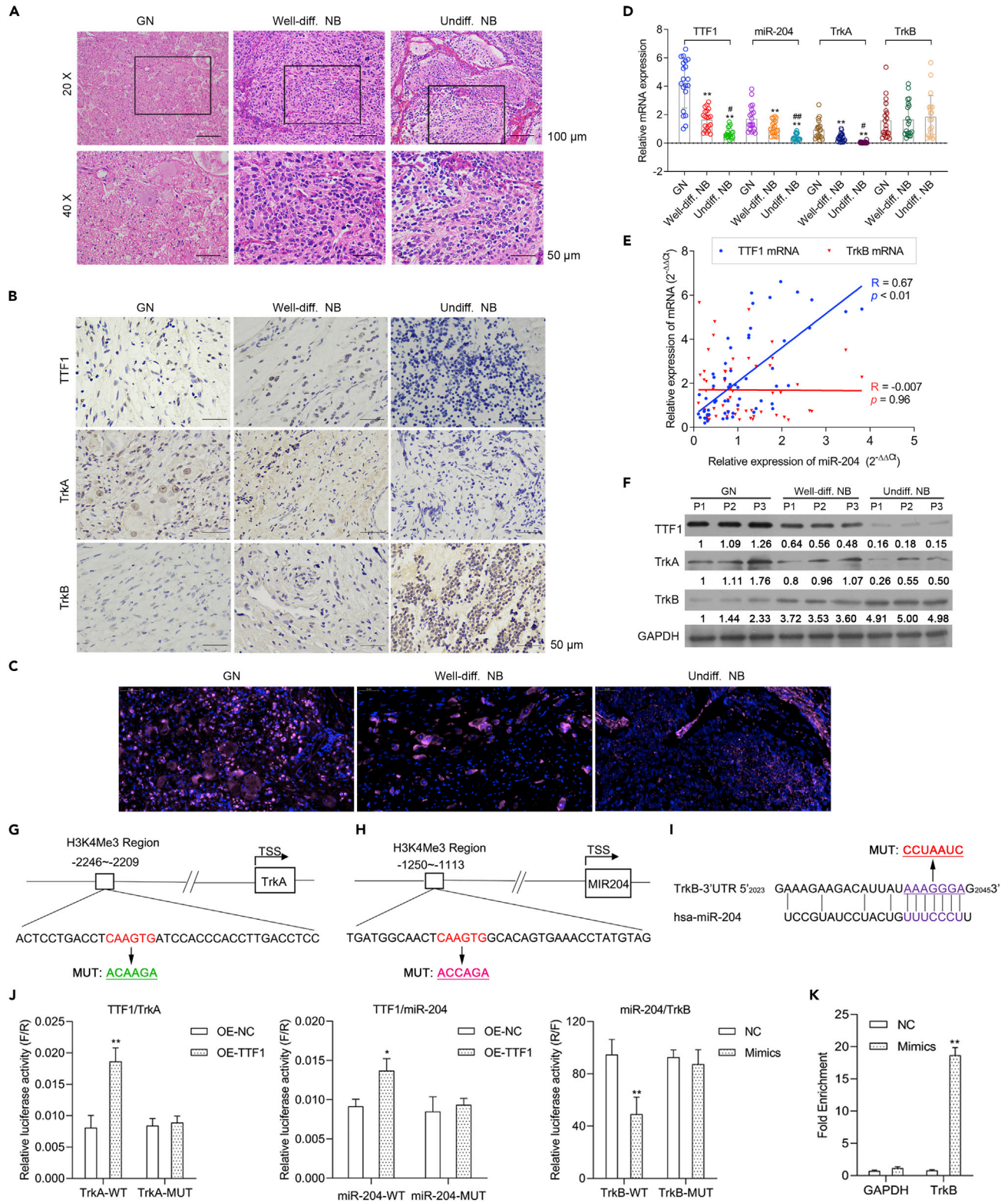
Figure 2. Expression and correlation analysis of TTF1, TrkA, TrkB, and miR-204 in GN, well-differentiated NB, and undifferentiated NB

(A) H&E staining of GN, well-differentiated NB, and undifferentiated NB tissues. Magnification, 20×; scale bar = 100 μm; magnification, 40×; scale bar = 50 μm.

(B) TTF1, TrkA, and TrkB levels in GN, well-differentiated NB, and undifferentiated NB were determined using IHC. Magnification, 40×; scale bar = 50 μm.

(C) MiR-204 expression in GN, well-differentiated NB, and undifferentiated NB tissue was detected using FISH. Magnification, 20 or 40 ×.

(D) TTF1, miR-204, TrkA, and TrkB expression in GN, well-differentiated NB, and undifferentiated NB determined using RT-qPCR.

(E) Correlation between miR-204 and TTF1, and miR-204 and TrkB.

(F) TTF1, TrkA, and TrkB expression in GN, well-differentiated NB, and undifferentiated NB tissues determined using Western blot.

(G–I) Predicted binding sites between TTF1 and the promoter of TrkA between TTF1 and the promoter of miR-204, and between miR-204 and 3'UTR of TrkB.

(J) Direct target relationships between TTF1 and the promoter of TrkA, between TTF1 and the promoter of miR-204, and between miR-204 and 3'UTR of TrkB were determined using luciferase reporter assays.

(K) RIP was conducted to verify the combination of miR-204 and TrkB. Data are represented as mean ± SD. *$p < 0.05$, **$p < 0.01$ vs. GN; #$p < 0.05$, ##$p < 0.01$ vs. well-differentiated NB.

Expression and correlation analysis of TTF1, TrkA, TrkB, and miR-204 in NB

Next, we collected GN, well-differentiated NB, and undifferentiated NB tissues (n = 20, respectively) from an independent cohort of NB patients to determine the expression and correlation between TTF1, TrkA, and TrkB. H&E staining revealed that GN rarely invaded the surrounding tissue and displayed regular cell polarity; however, well-differentiated and undifferentiated NB were likely to invade the surrounding tissues and exhibited pathologic multinucleation and loss of cell polarity, particularly in undifferentiated NB (Figure 2A). IHC showed that TTF1 and TrkA protein expression were dramatically lower in undifferentiated NB tissues, whereas TrkB expression was higher (Figure 2B). Next, we verified the expression of miR-204 in GN, undifferentiated, and well-differentiated NB using FISH. As shown in Figure 2C, miR-204 fluorescence was predominantly localized in the cytoplasm, whereas miR-204 expression was clearly lower in well-differentiated NB than in GN and even lower in undifferentiated NB than in well-differentiated NB. RT-qPCR revealed that *TTF1* and *TrkA* expression were significantly lower in differentiated and undifferentiated NB than in GN tissues, whereas *TrkB* did not differ (Figure 2D). A significant positive correlation between miR-204 and *TTF1* mRNA expression was observed in independent cohorts from the three groups (Figure 2E), while Western blot analysis confirmed the trends in TTF1 and TrkA expression identified using RT-qPCR. Notably, TrkB protein levels were dramatically higher in differentiated and undifferentiated NB than in GN tissues (Figure 2F).

Subsequent bioinformatics analyses identified potential TTF1 binding sites in the upstream transcriptional start site of TrkA (−2246 ∼ −2209 bp) and miR-204 (−1250 ∼ −1113 bp; Figures 2G and 2H). Moreover, luciferase reporter assays demonstrated that TTF1 overexpression significantly increased the luciferase activity of pGL3-WT-TrkA and pGL3-WT-miR-204 (Figure 2I). TargetScan predicted a potential miR-204 binding site in the 3'UTR of TrkB (Figure 2I). Consistently, we found that miR-204 overexpression remarkably suppressed the luciferase activity of TrkB-WT but not TrkB-MUT (Figure 2J), while RIP assays verified that miR-204 regulated TrkB (Figure 2K). Together, these data indicate that TrkA and miR-204 could be transcriptional targets of TTF1, and that TrkB is a direct target gene of miR-204.

TTF1 promoter methylation decreases TTF1 expression in NB

To identify TTF1 promoter methylation in NB, we performed pyrosequencing analysis and MSP. Although TTF1 promoter was methylated in GN, well-differentiated NB, and undifferentiated NB samples, TTF1 promoter methylation was more prominent in well-differentiated and undifferentiated NB tissues, particularly in undifferentiated NB tissues. Notably, TTF1 promoter methylation downregulated TTF1 expression in patients with undifferentiated NB (Figures S2A and S2C). Next, we measured TTF1 promoter methylation in SK-N-BE (TrkA-TrkB+) and SK-N-SH (TrkA+TrkB-) cells, finding that the TTF1 promoter was less methylated in SK-N-SH cells with high TrkA expression than in SK-N-BE cells with low TrkA expression (Figures S2B and S2D). Thus, these data suggest that TTF1 promoter methylation might decrease TTF1 and TrkA expression.

Effects of TTF1 on cell proliferation, apoptosis, and autophagy in NB cell lines

Next, we examined the regulatory effects of TTF1 overexpression or knockdown on the biological functions of SK-N-SH, IMR-32 (TrkA$^+$TrkB$^-$), SK-N-BE (TrkA$^-$TrkB$^+$), and SH-SY5Y (TrkA$^-$TrkB$^-$) cells. First, we silenced TTF1 in SK-N-SH and IMR-32 cells, and overexpressed TTF1 in SK-N-BE and SH-SY5Y cells. RT-qPCR revealed that TTF1 knockdown markedly downregulated TTF1 and TrkA, but did not affect TrkB expression in SK-N-SH and IMR-32 cells. Conversely, TTF1 overexpression clearly upregulated TTF1 and TrkA, but did
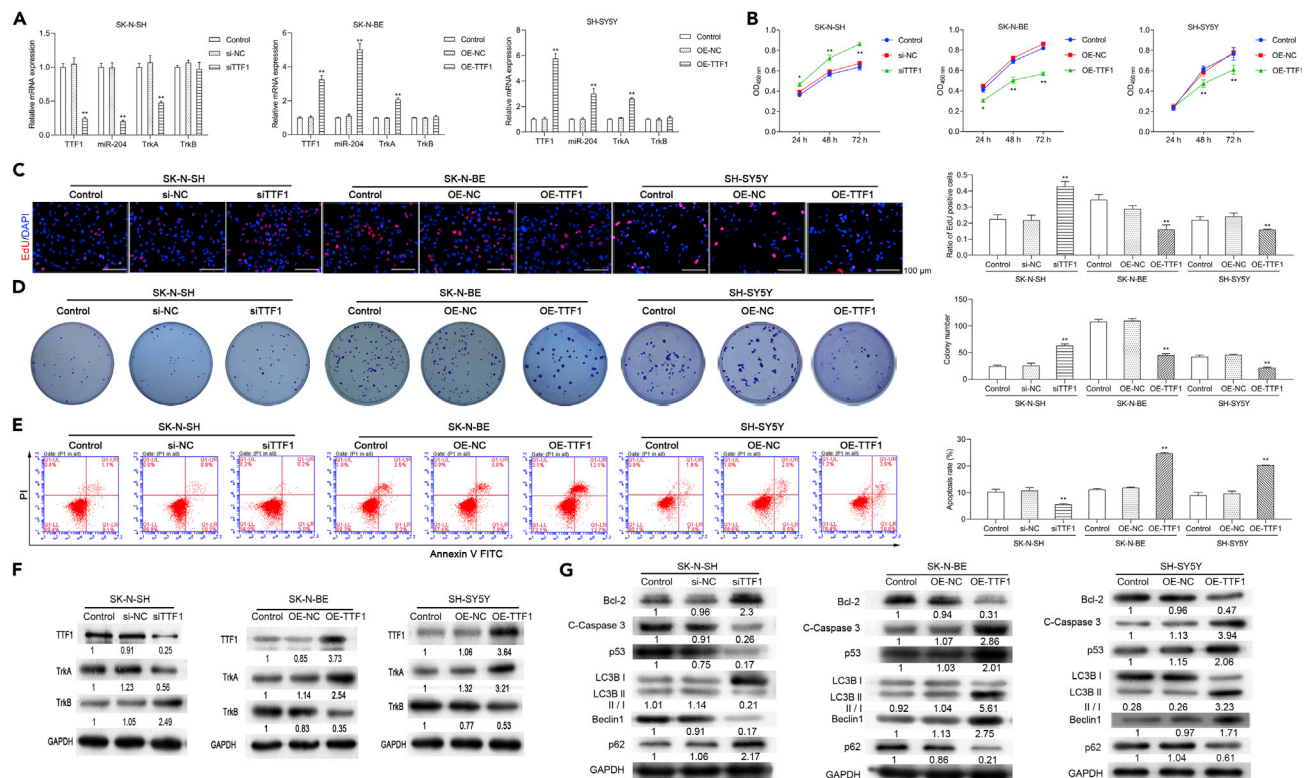
Figure 3. Effects of TTF1 on cell proliferation, apoptosis, and autophagy in SK-N-SH, SK-N-BE, and SH-SY5Y cells

(A–D) SK-N-SH cells were transfected with si-TTF1 and si-NC, while SK-N-BE and SH-SY5Y cells were transfected with pcDNA 3.1-TTF1 (OE-TTF1) and pcDNA-NC (OE-NC), respectively. (A) TTF1, miR-204, TrkA, and TrkB mRNA expression was determined using RT-qPCR in transfected SK-N-SH, SK-N-BE, and SH-SY5Y cells. Cell proliferation was assessed using (B) CCK-8, (C) EdU, and (D) colony formation assays.

(E) Apoptosis was detected and calculated using flow cytometry.

(F) TTF1, TrkA, and TrkB protein expression were determined using Western blot.

(G) Bcl-2, cleaved caspase-3 (C-caspase3), p53, LC3B-I, LC3B-II, Beclin1, and p62 levels were assessed using Western blot in the transfected SK-N-SH, SK-N-BE, and SH-SY5Y cells. Data are represented as mean ± SD. *$p < 0.05$, **$p < 0.01$.

not significantly alter TrkB expression in SK-N-BE and SH-SY5Y cells. MiR-204 was upregulated in TTF1-overexpressing SK-N-BE and SH-SY5Y cells and downregulated in TTF1-silenced SK-N-SH and IMR-32 cells (Figures 3A and S3A), whereas IF assays further showed that silencing TTF1 downregulated TrkA and up-regulated TrkB in IMR-32 cells (Figure S3B).

Subsequent CCK-8 and EdU staining showed that TTF1 overexpression significantly suppressed the pro-liferation of SK-N-BE and SH-SY5Y cells, whereas TTF1 knockdown accelerated the proliferation of SK-N-SH and IMR-32 cells (Figures 3B, 3C and S3D). Moreover, colony formation was significantly suppressed by TTF1 overexpression in SK-N-BE and SH-SY5Y cells, but significantly facilitated by TTF1 knockdown in SK-N-SH and IMR-32 cells (Figures 3D and S3E). Flow cytometry analysis of cell apoptosis further revealed that TTF1 overexpression increased the proportion of apoptotic SK-N-BE and SH-SY5Y cells, whereas TTF1 silencing decreased the number of apoptotic SK-N-SH and IMR-32 cells (Figures 3E and S3F). In addition, TTF1 overexpression induced cell cycle G0/G1 arrest, as indicated by an increase in the percentage of SK-N-BE and SH-SY5Y cells in G0/G1 phase, whereas TTF1 knockdown dramatically inhibited G0/G1 arrest in SK-N-SH and IMR-32 cells (Figures S4A, S4D, and S3G). Wound healing and Transwell assays revealed that TTF1 overexpression significantly suppressed the migration and invasion of SK-N-BE and SH-SY5Y cells, while TTF1 knockdown promoted the migration and invasion of SK-N-SH and IMR-32 cells (Figures S4B, S4C, S4E, S4F, S3C, and S3H). TEM further demonstrated that TTF1 overexpression enhanced autophagy in SK-N-BE and SH-SY5Y cells and that TTF1 silencing prevented autophagy in SK-N-SH cells (Figure S4G). Western blot confirmed that TTF1 overexpression markedly increased TrkA expression and decreased TrkB expression in SK-N-BE and SH-SY5Y cells; however, TTF1 knockdown dramatically decreased TrkA expres-sion and increased TrkB expression in SK-N-SH and IMR-32 cells (Figures 3F and S3I). Furthermore, Western
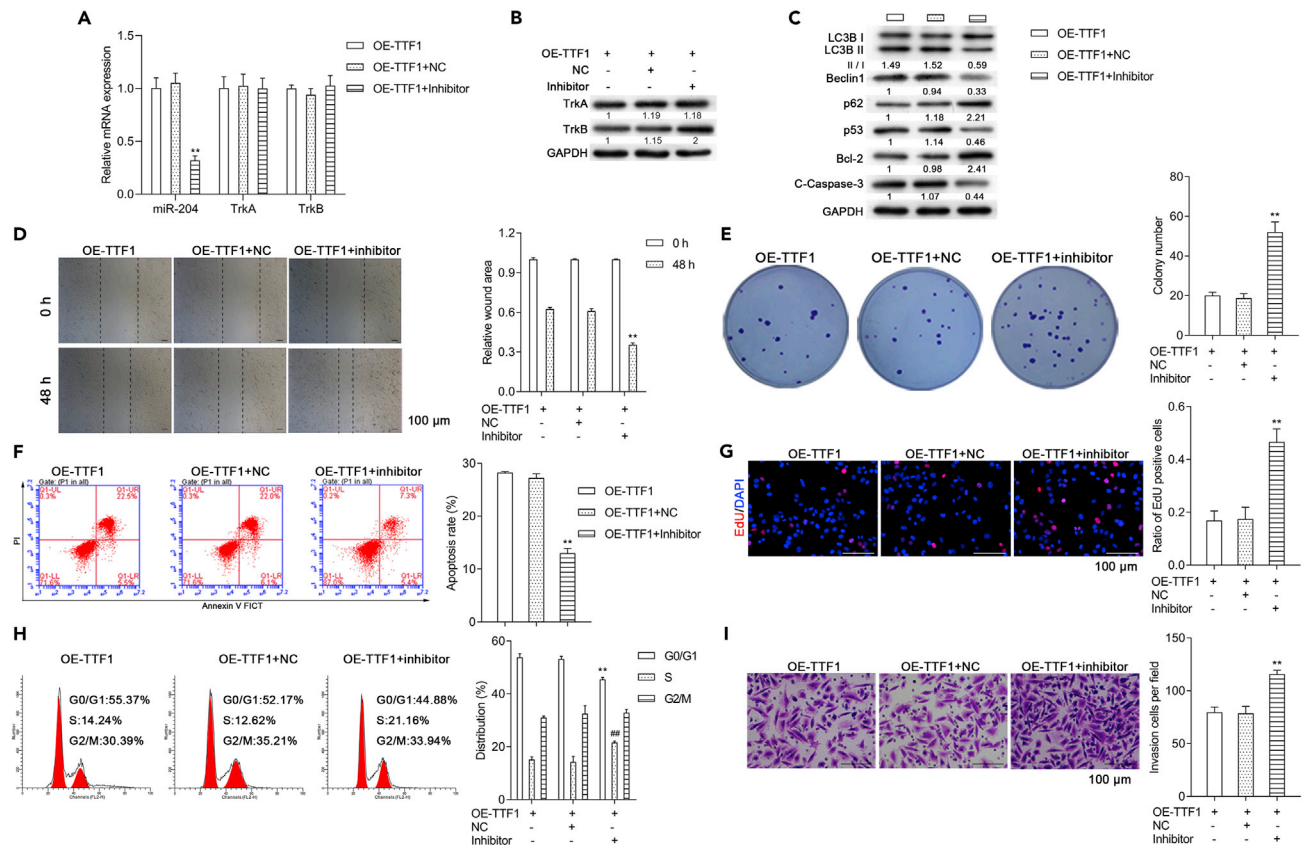
Figure 4. MiR-204 inhibition reverses TTF1 overexpression-mediated proliferation, apoptosis, cycle arrest, migration, invasion, and autophagy in SK-N-BE cells

SK-N-BE cells were co-transfected with TTF1-overexpression plasmids and a miR-204 inhibitor.

(A) MiR-204, TrkA, and TrkB expression was confirmed using RT-qPCR.

(B) TrkA and TrkB protein expression was identified using Western blot.

(C) LC3B-I, LC3B-II, Beclin1, p62, p53, Bcl-2, and C-Caspase3 protein expression was detected by Western blot in SK-N-BE cells after co-transfection.

(D) Migration was measured using wound healing assays.

(E) Cell proliferation was assessed using colony formation assays in co-transfected SK-N-BE cells.

(F) Cell apoptosis was monitored and quantified using flow cytometry.

(G) Cell proliferation was monitored using EdU staining.

(H) Cell cycle distribution was determined using flow cytometry.

(I) Invasion was investigated using Transwell assays. Magnification, 20×. Data are represented as mean ± SD. **$p < 0.01$, ##$p < 0.01$.

blot analysis revealed that TTF1 overexpression promoted apoptosis and autophagy in SK-N-BE and SH-SY5Y cells by downregulating Bcl-2 and p62, and upregulating C-Caspase-3, p53, and LC3B-II/I. Conversely, silencing TTF1 repressed SK-N-SH and IMR-32 cell apoptosis and autophagy by upregulating Bcl-2 and p62, and downregulating C-Caspase-3, p53, and LC3B-II/I (Figures 3G and S3J). Taken together, these findings indicate that TTF1 overexpression inhibits cell cycle progression, migration, and invasion, and induces apoptosis and autophagy in SK-N-BE and SH-SY5Y cells, whereas TTF1 knockdown exerts the opposite effects in SK-N-SH and IMR-32 cells.

MiR-204 inhibition reverses the effects of TTF1 overexpression in SK-N-BE cells

To determine whether miR-204 is a key downstream regulator via which TTF1 regulates the functions of NB cells, we co-transfected SK-N-BE cells with TTF1-overexpression plasmids and miR-204 inhibitors. As expected, miR-204 was downregulated in SK-N-BE cells co-transfected with the TTF1-overexpression plasmid and miR-204 inhibitor, whereas TrkB expression was slightly upregulated (Figure 4A). Meanwhile, miR-204 inhibition dramatically upregulated TrkB in TTF1-overexpressed SK-N-BE cells (Figure 4B). Western blot analysis further revealed that miR-204 inhibition downregulated LC3-II/I ratio, Beclin1, p53, and C-caspase-3, and upregulated p62 and Bcl-2 in TTF1-overexpressed SK-N-BE cells, indicating that
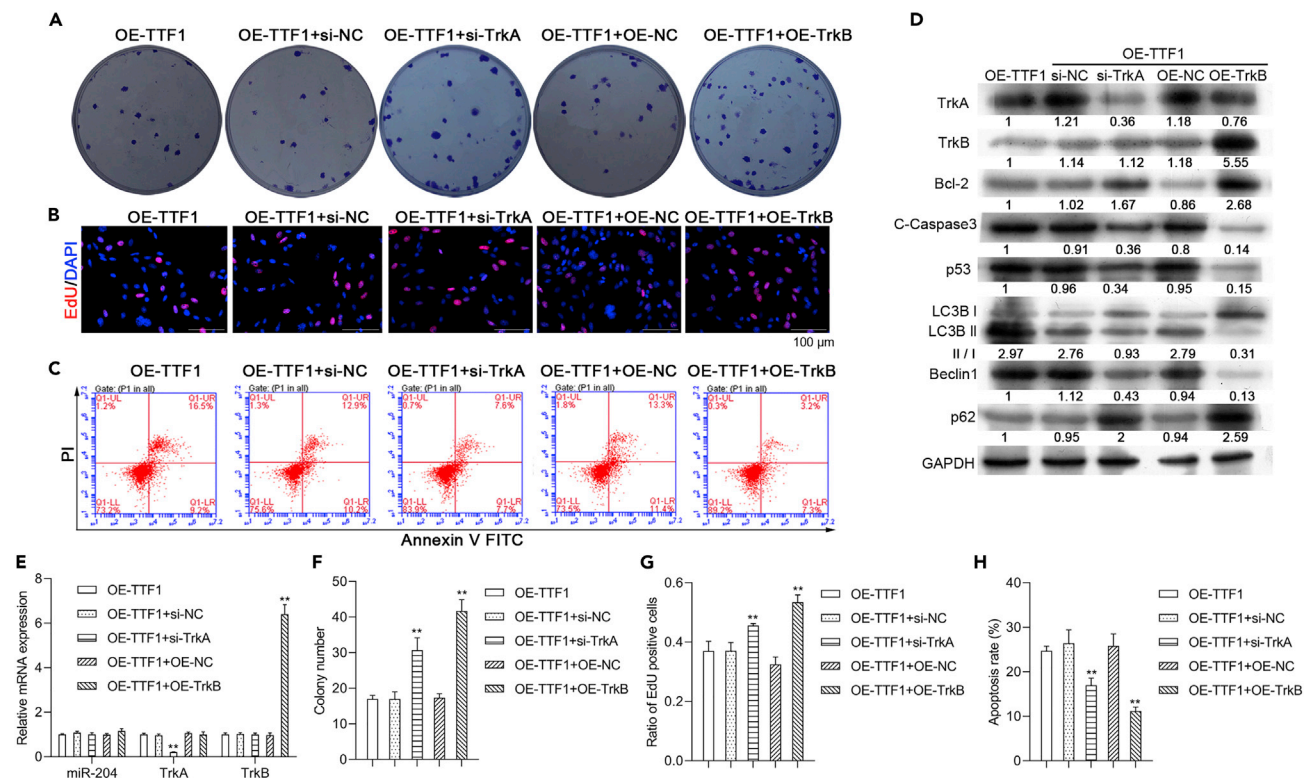
Figure 5. TrkA silencing and TrkB overexpression reverses SK-N-BE cell proliferation suppression, apoptosis, and autophagy mediated by TTF1 overexpression

SK-N-BE cells were co-transfected with TTF1-overexpression plasmids and TrkA siRNAs or TrkB-overexpression plasmids, respectively.

(A and B) Cell proliferation was identified using (A) colony formation and (B) EdU assays in co-transfected SK-N-BE cells.

(C) Apoptosis was measured using flow cytometry in SK-N-BE cells after co-transfection.

(D) TrkA, TrkB, Bcl-2, C-Caspase3, p53, LC3B-I, LC3B-II, Beclin1, and p62 expression was measured using Western blot analysis in co-transfected SK-N-BE cells.

(E) MiR-204, TrkA, and TrkB expression was measured using RT-qPCR in co-transfected SK-N-BE cells.

(F–H) The (F) colony number, (G) ratio of EdU positive cells, and (H) apoptosis rate were quantified based on the respective results.

Data are represented as mean $\pm$ SD. $**p < 0.01$.

miR-204 inhibition attenuated cell apoptosis and autophagy induced by TTF1 overexpression in SK-N-BE cells (Figure 4C). In addition, colony formation assays confirmed that miR-204 inhibition significantly promoted cell proliferation in TTF1-overexpressing SK-N-BE cells (Figure 4E), whereas EdU staining revealed the same trend for SK-N-BE cell proliferation (Figure 4G). Consistently, miR-204 inhibition markedly suppressed apoptosis (Figure 4F) and cell-cycle arrest (Figure 4H) in TTF1-overexpressing SK-N-BE cells while facilitating their migration (Figure 4D) and invasion (Figure 4I). Together, these findings show that TTF1 inhibits the malignant behaviors of SK-N-BE cells by targeting miR-204.

TrkA silencing and TrkB overexpression reverse the effects of TTF1 overexpression in SK-N-BE cells

To further explore whether TTF1 acts via TrkA and TrkB, we transfected SK-N-BE cells with TTF1-overexpression plasmids alone or with TrkA siRNAs or TrkB-overexpression plasmids. Notably, TrkA knockdown or TrkB overexpression dramatically enhanced SK-N-BE cell proliferation even in SK-N-BE cells co-transfected with TTF1 overexpression plasmid (Figures 5A and 5F), as confirmed using EdU, cell proliferation, and colony formation assays (Figures 5B and 5G). Moreover, TrkA knockdown or TrkB overexpression reversed the increased apoptosis induced by TTF1 overexpression in SK-N-BE cells (Figures 5C and 5H). Western blot analysis confirmed that TrkA knockdown or TrkB overexpression downregulated TrkA, C-Caspase-3, p53, LC3B-II/I ratio, and Beclin1, and upregulated TrkB, Bcl-2, and p62 in TTF1-overexpressing SK-N-BE cells (Figure 5D). The successful transfection of TTF1-overexpressing SK-N-BE cells with TrkA siRNAs or TrkB-overexpression plasmid was confirmed using RT-qPCR (Figure 5E). Thus, these findings
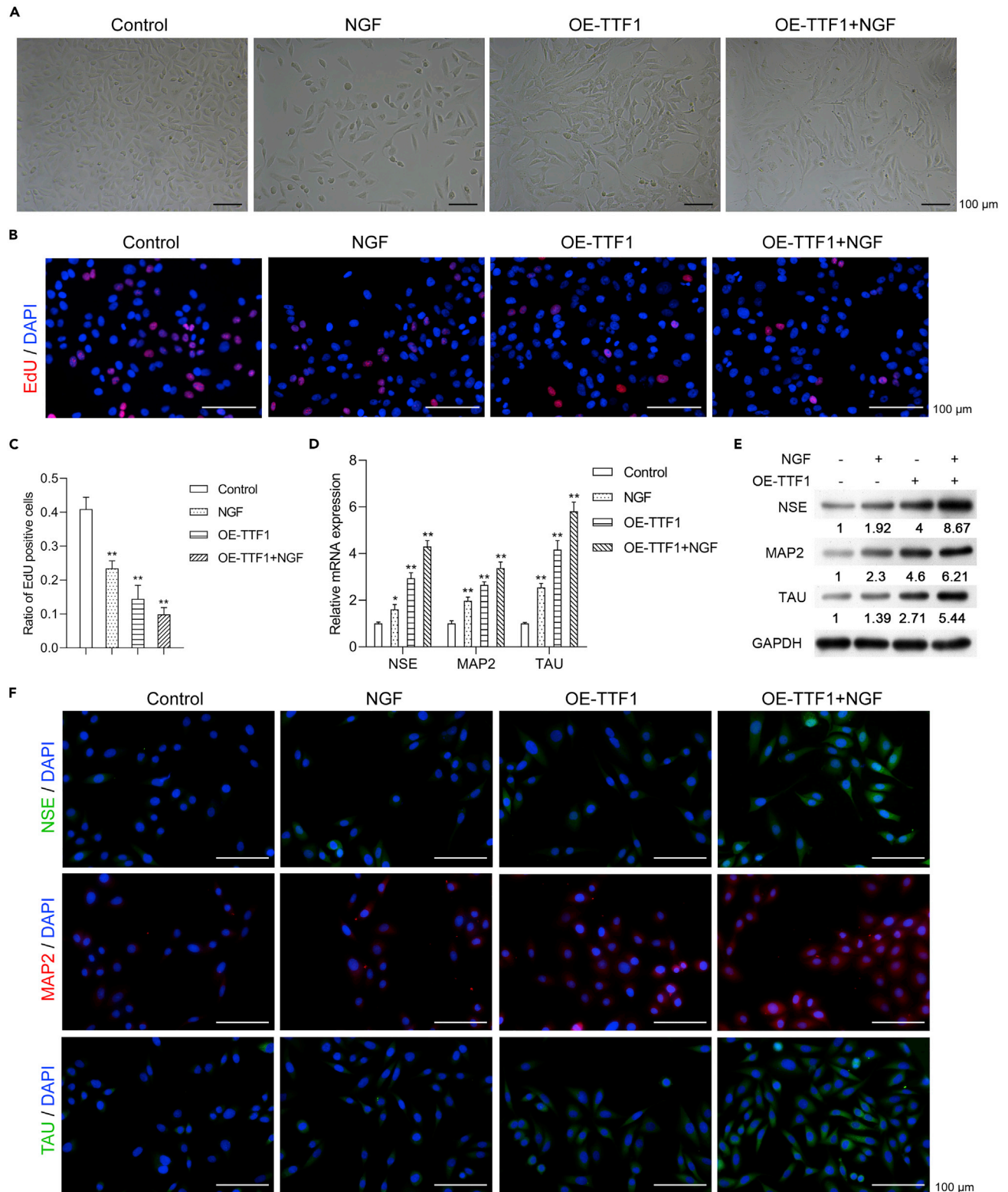
Figure 6. TTF1 promotes the neurogenic differentiation of SK-N-BE cells under NGF stimulation

SK-N-BE cells were pre-treated with NGF and transfected with TTF1-overexpression plasmids.

(A) Cellular morphology was observed under a light microscope.

Figure 6. *Continued*
(B) Cell proliferation was detected using EdU staining assays. Magnification, 20✕.
(C) The ratio of EdU positive cells was counted. NSE, MAP2, and TAU levels were determined using (D) RT-qPCR, (E) Western blot, and (F) IF staining.
Magnification, 20✕. Data are represented as mean ± SD. *p < 0.05, **p < 0.01.

show that silencing TrkA or overexpressing TrkB could reverse the suppression of proliferation and suppress apoptosis and autophagy mediated by TTF1 overexpression in SK-N-BE cells.

TTF1 promotes neurogenic differentiation in NGF-treated SK-N-BE cells

Next, we evaluated the effects of TTF1 on NB cell differentiation by pre-treating SK-N-BE cells with NGF and transfecting them with TTF1-overexpression plasmids. Morphologically, NB cells transfected with the TTF1-overexpression plasmid and treated with NGF showed a slender spindle type and a smaller cell nucleus than those in cells with the NGF treatment or TTF1-overexpression alone (Figure 6A). The percentage of EdU-positive cells decreased after NGF treatment or TTF1-overexpression, and further decreased in TTF1-overexpressing SK-N-BE cells with NGF treatment (Figures 6B and 6C). In addition, we evaluated the expression levels of differentiation markers, including neuron-specific enolase (NSE), microtubule-binding proteins like microtubule-associated protein 2 (MAP2), and microtubule-associated protein tau (TAU). Both RT-qPCR (Figure 6D) and Western blot (Figure 6E) confirmed that NSE, MAP2, and TAU expression increased after either NGF or TTF1-overexpression, but increased more significantly after co-treatment with TTF1-overexpression plasmids and NGF, as confirmed by immunofluorescence assays (Figure 6F). Hence, we verified that TTF1 could induce neurogenic differentiation in SK-N-BE cells after NGF stimulation.

TTF1 suppresses tumor growth *in vivo*

We next examined whether TTF1 overexpression could suppress NB tumor growth *in vivo* using a subcutaneous xenograft mouse model established by NC- or TTF1-transfected SK-N-BE cells. As depicted in Figures 7A and 7B, tumors formed from TTF1-overexpressing SK-N-BE cells were significantly smaller at 28 days after inoculation. Time-dependent analysis revealed that tumor volume was remarkably suppressed in mice inoculated with TTF1-overexpressing cells (Figure 7C). RT-qPCR further showed that miR-204 was upregulated in the TTF1-overexpression group (Figure 7D), while IHC (Figures 7E and 7F) and Western blot analysis (Figure 7G) indicated that TTF1 and TrkA expression increased and TrkB decreased in the TTF1-overexpression group. Moreover, the expression of autophagy markers including LC3B, p62, and p53 were significantly upregulated in tumor tissues from TTF1 overexpression NB cells.

TTF1 induces neurogenic differentiation *in vivo*

Finally, we evaluated the effects of TTF1 on neurogenic differentiation *in vivo* using a xenograft mouse model established using SK-N-BE cells (NC, NGF treatment, or TTF1 overexpression and NGF treatment). Notably, NGF treatment alone was able to moderately inhibit tumor growth compared to NC; however, NGF treatment in TTF1-overexpressing cells caused significant regression compared to NGF alone (Figures 8A–8C). IHC analysis of tumor tissue confirmed increased TTF1, TrkA, MAP2, NSE, and TAU, but decreased TrkB expression in the NGF group compared to the NC group (Figures 8D and 8E), while Western blot demonstrated a similar trend in TTF1, TrkA, TrkB, MAP2, NSE, and TAU expression (Figure 8F). Taken together, these data demonstrate that TTF1 overexpression with NGF treatment could promote neurogenic differentiation *in vivo*.

DISCUSSION

In this study, we identified and validated ten miRNAs associated with NB differentiation, including five downregulated miRNAs (miR-206, miR-34b, miR-489, miR-204, and miR-653) and five upregulated miRNAs (miR-513c, miR-203, miR-216a, miR-4484, and miR-148a). Among the downregulated miRNAs, miR-204 had the lowest expression level in undifferentiated NB tissues compared to well-differentiated NB and GN tissues. Therefore, we predicted up- and down-stream regulators of miR-204 using bioinformatics software and confirmed their relationship using luciferase reporter assays. Interestingly, we found that TTF1 directly targeted TrkA and miR-204, and that TrkB was a direct target of miR-204. The associations between TTF1, TrkA, miR-204, and TrkB during NB differentiation and progression were then explored using gain- and loss-of-function assays. TTF1 overexpression induced cell cycle arrest, apoptosis, and autophagy, and suppressed migration and invasion in SK-N-BE (TrkA⁻TrkB⁺) and SH-SY5Y (TrkA⁻TrkB⁻) cells, while TTF1
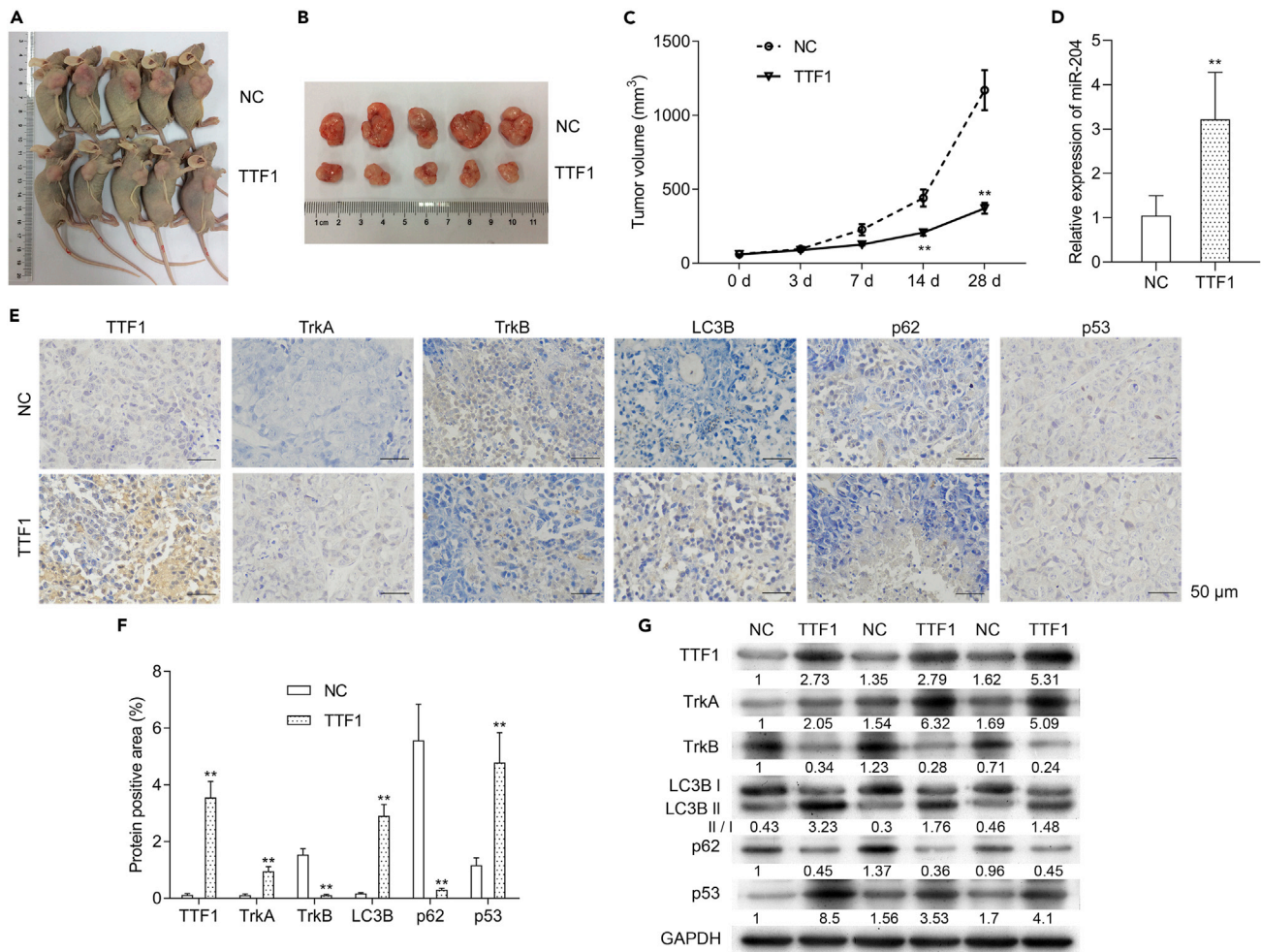
Figure 7. TTF1 suppresses NB tumor growth *in vivo*. Nude mice were subcutaneously injected with 2×10^6 SK-N-BE cells transfected with NC or TTF1-overexpression plasmids

(A) Subcutaneous xenograft nude mouse model.

(B) Representative images of tumors in mice injected with NC or TTF1-transfected SK-N-BE cells.

(C) Tumor volume on days 0, 3, 7, 14, and 28 after injection.

(D) MiR-204 levels in NB tissue were analyzed using RT-qPCR.

(E and F) TTF1, TrkA, TrkB, LC3B, p62, and p53 protein expression was determined using IHC staining. Positive cells were counted. Magnification, 20×; scale bar = 50 μm.

(G) TTF1, TrkA, TrkB, LC3B, p62, and p53 expression in NB tissues was analyzed using Western blot. Data are represented as mean ± SD. **p < 0.01 vs. NC.

knockdown exerted the opposite effects in SK-N-SH and IMR-32 cells (TrkA[+]TrkB[−]). Together, these data confirm that TTF1 acts as a tumor suppressor in NB progression.

Previous studies have suggested that TTF1 is a dual function lineage factor that can exert opposing effects in cancer cells. For instance, Phelps et al. (2018) showed that TTF1 can have either oncogenic or tumor suppressive activities, despite the fact that TTF1 undergoes gene amplification in lung cancer. Similarly, Yamaguchi et al. (2013) reported that TTF1 is characteristically overexpressed in terminal respiratory unit-type adenocarcinomas and functions as a 'lineage-survival' oncogene in lung adenocarcinomas. Ueda et al. (2015) noted that patients with colorectal cancer with high TTF1 expression had a significantly poorer prognosis than those with low TTF1 expression. Consistent with our findings, conditional TTF1 knockout was reported to enhance the development of invasive K-ras-driven mucinous lung adenocarcinoma (Winslow et al., 2011) and TTF1 has been shown to inhibit HUVEC tube formation and HepG2 cell migration and invasion, and inhibit tumor growth in nude mice implanted with HepG2 cells (Xiao et al., 2016).
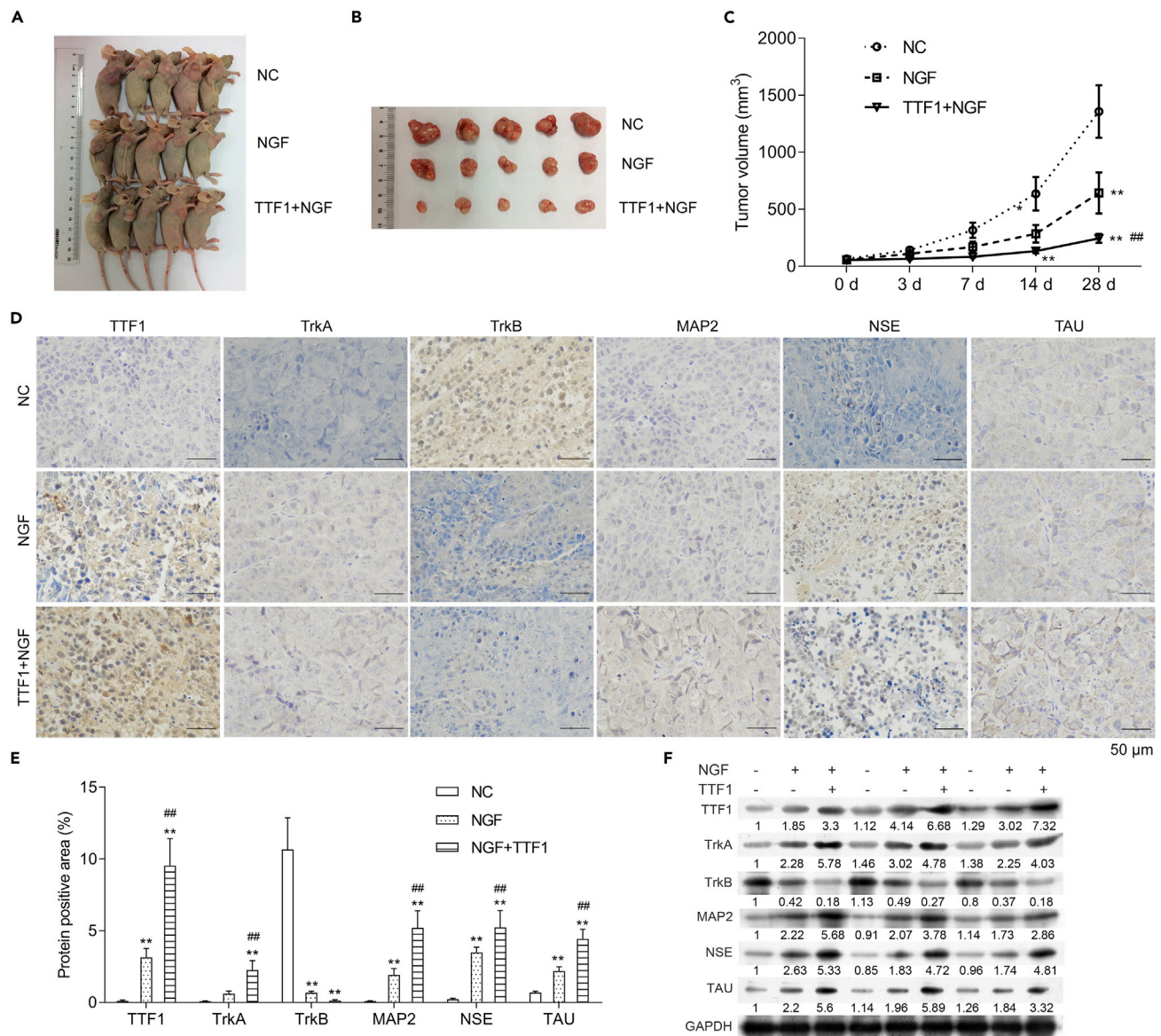
Figure 8. TTF1 induces neurogenic differentiation *in vivo*

Nude mice were subcutaneously injected with 2 × 10⁶ SK-N-BE cells with NGF overexpression and simultaneous NGF and TTF1 overexpression.

(A) Subcutaneous xenograft nude mouse model.

(B) Representative images of tumors in nude mice injected with SK-N-BE cells.

(C) Tumor volume on days 0, 3, 7, 14, and 28 after injection.

(D–F) TTF1, TrkA, TrkB, MAP2, NSE, and TAU protein expressions were determined using IHC staining and Western blot. Magnification, 20×; scale bar = 50 μm. Data are represented as mean ± SD. *p < 0.05, **p < 0.01 vs. NC; ##p < 0.01 vs. NGF.

In this study, we also discovered that TTF1 simultaneously suppresses NB tumor growth and induces neurogenic differentiation *in vitro* and *in vivo*. Accumulating evidence has suggested that increased neuronal differentiation is strongly associated with decreased tumor growth in NB. For instance, Bruno et al. (2020) showed that β3-adrenergic receptor antagonist (SR59230A) inhibits NB growth and tumor progression by causing a switch from stemness to cell differentiation *in vivo* and *in vitro*. Chen et al. (2019) also reported that Krüppel-like factor 9 (KLF9) exerts pro-differentiation and growth-inhibition effects in NB. At the molecular level, we confirmed that TTF1 overexpression increased the expression of NGF-induced neuronal marker genes, such as NSE, MAP2, and TAU. Differentiating NB has a less aggressive phenotype and a favorable prognosis, whereas poorly or undifferentiated NB is characterized by rapid tumor progression and a

low overall survival rate (Cohn et al., 2009; Shimada et al., 1995, 2001). TrkA is a detergent soluble fraction component that has been reported to mediate NB cell differentiation (Chiricozzi et al., 2019). Notably, the NGF/TrkA axis was found to promote NB differentiation and regression, whereas the BDNF/TrkB axis was responsible for NB cell survival and angiogenesis and maintaining undifferentiated NB cells (Khotskaya et al., 2017; Pacenta and Macy, 2018). Because TTF1 has been reported to potentially promote lung carcinoma differentiation (Winslow et al., 2011), we hypothesized that TTF1 could induce NB neurogenic differentiation by regulating TrkA and TrkB, consistent with the findings of our *in vitro* and *in vivo* experiments.

We also identified miR-204 as a transcriptional target of TTF1 that was directly regulated by TTF1 by binding to a genomic region located 1113–1250 bp upstream of miR-204. TTF1 expression correlated positively with miR-204 levels in three independent groups of patients with NB, while *in vitro* experiments demonstrated that downregulating miR-204 reversed the biological effects of TTF1 overexpression on the proliferation, cell cycle distribution, migration, invasion, apoptosis, and autophagy in SK-N-BE cells. Thus, miR-204 appears to be a key regulator of TTF1 in NB progression by acting as a differentiation-related tumor suppressor. It has been recently reported that miR-532-5p is a transcriptional target of TTF1 with a tumor suppressive role in lung adenocarcinoma cells (Griesing et al., 2017), while the targeted regulation of miR-7 expression via the TTF1 promoter significantly inhibited the growth of human lung cancer (Lei et al., 2017). Indeed, multiple previous studies have found that miR-204 is frequently downregulated in cancer and acts as tumor suppressor during tumorigenesis (Cui et al., 2014; Guo et al., 2019; Saadi et al., 2012; Wang et al., 2015). Several studies have demonstrated a functional link between NB and miR-204, which predicts favorable clinical outcome at least in part by increasing cisplatin sensitivity by targeting Bcl-2 (Ryan et al., 2012). MiR-204 has also been identified as a direct inhibitor of MYCN (Ooi et al., 2018) and PHOX2B (Bachetti et al., 2015) in NB. In this study, we identified TrkB as a direct target gene of miR-204 in NB cells. Based on the potential role of miR-204 in inducing the differentiation of glioma stem-like cells (Ying et al., 2013), it is reasonable to hypothesize that TTF1 negatively regulates TrkB expression by targeting miR-204 to induce neurogenic differentiation and inhibit tumor growth.

In summary, our study identified miR-204 as a NB differentiation-related factor and found that TTF1 acts as a functional tumor suppressor in NB by promoting neurogenic differentiation *in vitro* and *in vivo*. Furthermore, we found that TTF1 directly targets TrkA and the miR-204/TrkB axis to exert antitumor effects in NB (graphical abstract). Consequently, we believe that the TTF1/miR-204/TrkB axis might provide a theoretical basis for effective targeted therapy and novel drugs against NB.

Limitations of the study

In this study, we found that TTF1 suppresses NB growth and induces NB differentiation by targeting TrkA and the miR-204/TrkB axis. TTF1 promoted the neurogenic differentiation both *in vitro* and *in vivo*. However, studies on the mechanisms by which TTF1 regulates differentiation are needed. Here we only proved that regulation of the TrkA and miR-204/TrkB axes by TTF1 is linked to cell proliferation and death, but not to differentiation directly. In addition, more detailed evidence should be provided to validate that TTF1 negatively regulates TrkB expression by targeting miR-204. Furthermore, *in vivo* study only proved that TTF1 suppresses tumor growth and induces neurogenic differentiation. The exact role of miR-204 *in vivo* needs to be further explored.

STAR★METHODS

Detailed methods are provided in the online version of this paper and include the following:

- KEY RESOURCES TABLE
- RESOURCE AVAILABILITY
  - Lead contact
  - Materials availability
  - Data and code availability
- EXPERIMENTAL MODEL AND SUBJECT DETAILS
  - Patients and samples
  - Cell lines
  - Animal studies
- METHOD DETAILS
  - RNA-seq and gene expression omnibus (GEO) database analysis

- ○ MiRNA sequencing (miRNA-seq)
- ○ Bioinformatics analysis
- ○ Cell transfection
- ○ RT-qPCR
- ○ Fluorescence *in situ* hybridization (FISH)
- ○ Luciferase reporter assay
- ○ RNA immunoprecipitation (RIP) assay
- ○ DNA bisulphite treatment and methylation-specific PCR (MSP)
- ○ Flow cytometry analysis
- ○ Wound healing assay
- ○ Cell invasion assay
- ○ Transmission electron microscopy (TEM)
- ○ Immunofluorescence (IF) assay
- ○ CCK-8 assay
- ○ Colony formation assay
- ○ EdU assay
- ○ Western blot analysis
- ○ Immunohistochemistry (IHC)
- ● QUANTIFICATION AND STATISTICAL ANALYSIS

SUPPLEMENTAL INFORMATION

Supplemental information can be found online at https://doi.org/10.1016/j.isci.2022.104655.

AUTHOR CONTRIBUTIONS

T.Y., J.H., and H.X. conceptualized and designed the study. T.Y. and J.L. performed the experiments. Z.Z., H.Z., T.T., L.M., and M.Z. conducted bioinformatics analysis and experiment data analyses. J.Y., J.P., C.H., and Y.Z. collected tissue specimens and clinical data. T.Y., Z.Z., J.H., and H.X. wrote the paper. All authors read and approved the final manuscript.

DECLARATION OF INTERESTS

The authors declare no competing interests.

REFERENCES

Ackermann, S., Cartolano, M., Hero, B., Welte, A., Kahlert, Y., Roderwieser, A., Bartenhagen, C., Walter, E., Gecht, J., Kerschke, L., et al. (2018). A mechanistic classification of clinical phenotypes in neuroblastoma. Science *362*, 1165–1170. https://doi.org/10.1126/science.aat6768.

Aravindan, N., Subramanian, K., Somasundaram, D.B., Herman, T.S., and Aravindan, S. (2019). MicroRNAs in neuroblastoma tumorigenesis, therapy resistance, and disease evolution. Cancer Drug Resist. *2*, 1086–1105. https://doi.org/10.20517/cdr.2019.68.

Bachetti, T., Di Zanni, E., Ravazzolo, R., and Ceccherini, I. (2015). miR-204 mediates post-transcriptional down-regulation of PHOX2B gene expression in neuroblastoma cells. Biochim.

Biophys. Acta *1849*, 1057–1065. https://doi.org/10.1016/j.bbagrm.2015.06.008.

Bartel, D.P. (2004). MicroRNAs: genomics, biogenesis, mechanism, and function. Cell *116*, 281–297. https://doi.org/10.1016/s0092-8674(04)00045-5.

Brodeur, G.M. (2003). Neuroblastoma: biological insights into a clinical enigma. Nat. Rev. Cancer *3*, 203–216. https://doi.org/10.1038/nrc1014.

Brodeur, G.M. (2018). Spontaneous regression of neuroblastoma. Cell Tissue Res. *372*, 277–286. https://doi.org/10.1007/s00441-017-2761-2.

Brodeur, G.M., Iyer, R., Croucher, J.L., Zhuang, T., Higashi, M., and Kolla, V. (2014). Therapeutic

targets for neuroblastomas. Expert Opin. Ther. Targets *18*, 277–292. https://doi.org/10.1517/14728222.2014.867946.

Bruno, G., Cencetti, F., Pini, A., Tondo, A., Cuzzubbo, D., Fontani, F., Strinna, V., Buccoliero, A.M., Casazza, G., Donati, C., et al. (2020). β3-adrenoreceptor blockade reduces tumor growth and increases neuronal differentiation in neuroblastoma via SK2/S1P(2) modulation. Oncogene *39*, 368–384. https://doi.org/10.1038/s41388-019-0993-1.

Chen, S., Gu, S., Xu, M., Mei, D., Xiao, Y., Chen, K., and Yan, Z. (2019). Krüppel-like factor 9 promotes neuroblastoma differentiation via targeting the sonic hedgehog signaling pathway. Pediatr.

Blood Cancer 67, e28108. https://doi.org/10.1002/pbc.28108.

Chiricozzi, E., Biase, E.D., Maggioni, M., Lunghi, G., Fazzari, M., Pomè, D.Y., Casellato, R., Loberto, N., Mauri, L., and Sonnino, S. (2019). GM1 promotes TrkA-mediated neuroblastoma cell differentiation by occupying a plasma membrane domain different from TrkA. J. Neurochem. 149, 231–241. https://doi.org/10.1111/jnc.14685.

Cohn, S.L., Pearson, A.D., London, W.B., Monclair, T., Ambros, P.F., Brodeur, G.M., Faldum, A., Hero, B., Iehara, T., Machin, D., et al. (2009). The international neuroblastoma risk group (INRG) classification system: an INRG task force report. J. Clin. Oncol. 27, 289–297. https://doi.org/10.1200/JCO.2008.16.6785.

Cui, Z.H., Shen, S.Q., Chen, Z.B., and Hu, C. (2014). Growth inhibition of hepatocellular carcinoma tumor endothelial cells by miR-204-3p and underlying mechanism. World J. Gastroenterol. 20, 5493. https://doi.org/10.3748/wjg.v20.i18.5493.

Da, W.H., Sherman, B.T., and Lempicki, R.A. (2008). Systematic and integrative analysis of large gene lists using DAVID bioinformatics resources. Nat. Protoc. 4, 44–57. https://doi.org/10.1038/nprot.2008.211.

de Planell-Saguer, M., Rodicio, M.C., and Mourelatos, Z. (2010). Rapid in situ codetection of noncoding RNAs and proteins in cells and formalin-fixed paraffin-embedded tissue sections without protease treatment. Nat. Protoc. 5, 1061–1073. https://doi.org/10.1038/nprot.2010.62.

Espinoza, C.R., Schmitt, T.L., and Loos, U. (2001). Thyroid transcription factor 1 and Pax8 synergistically activate the promoter of the human thyroglobulin gene. J. Mol. Endocrinol. 27, 59–67. https://doi.org/10.1677/jme.0.0270059.

Fontana, L., Fiori, M.E., Albini, S., Cifaldi, L., Giovinazzi, S., Forloni, M., Boldrini, R., Donfrancesco, A., Federici, V., Giacomini, P., et al. (2008). Antagomir-17-5p abolishes the growth of therapy-resistant neuroblastoma through p21 and BIM. PLoS One 3, e2236. https://doi.org/10.1371/journal.pone.0002236.

Fung, W., Hasan, M.Y., Pheng Loh, A.H., Yiing Chua, J.H., Hwee, Y.M., Knight, L., Sek, H.W., Yoke, C.M., Tew, S.W., Jacobsen, A.S., and Hon, C.C. (2011). Gene expression of TRK neurotrophin receptors in advanced neuroblastomas in Singapore–a pilot study. Pediatr. Hematol. Oncol. 28, 571–578. https://doi.org/10.3109/08880018.2011.575443.

Griesing, S., Kajino, T., Tai, M.C., Liu, Z., Nakatochi, M., Shimada, Y., Suzuki, M., and Takahashi, T. (2017). Thyroid transcription factor-1-regulated microRNA-532-5p targets KRAS and MKL2 oncogenes and induces apoptosis in lung adenocarcinoma cells. Cancer Sci. 108, 1394–1404. https://doi.org/10.1111/cas.13271.

Guazzi, S., Price, M., De Felice, M., Damante, G., Mattei, M.G., and Di Lauro, R. (1990). Thyroid nuclear factor 1 (TTF-1) contains a homeodomain and displays a novel DNA binding specificity. EMBO J. 9, 3631–3639. https://doi.org/10.1002/j.1460-2075.1990.tb07574.x.

Guo, J., Zhao, P., Liu, Z., Li, Z., Yuan, Y., Zhang, X., Yu, Z., Fang, J., and Xiao, K. (2019). MiR-204-3p inhibited the proliferation of bladder cancer cells via modulating lactate dehydrogenase-mediated glycolysis. Front. Oncol. 9, 1242. https://doi.org/10.3389/fonc.2019.01242.

Khotskaya, Y.B., Holla, V.R., Farago, A.F., Mills Shaw, K.R., Meric-Bernstam, F., and Hong, D.S. (2017). Targeting TRK family proteins in cancer. Pharmacol. Ther. 173, 58–66. https://doi.org/10.1016/j.pharmthera.2017.02.006.

Kogner, P., Barbany, G., Dominici, C., Castello, M.A., Raschellà, G., and Persson, H. (1993). Coexpression of messenger RNA for TRK protooncogene and low affinity nerve growth factor receptor in neuroblastoma with favorable prognosis. Cancer Res. 53, 2044–2050.

Kondo, T., Nakazawa, T., Ma, D., Niu, D., Mochizuki, K., Kawasaki, T., Nakamura, N., Yamane, T., Kobayashi, M., and Katoh, R. (2009). Epigenetic silencing of TTF-1/NKX2-1 through DNA hypermethylation and histone H3 modulation in thyroid carcinomas. Lab. Invest. 89, 791–799. https://doi.org/10.1038/labinvest.2009.50.

Lei, L., Chen, C., Zhao, J., Wang, H., Guo, M., Zhou, Y., Luo, J., Zhang, J., and Xu, L. (2017). Targeted expression of miR-7 operated by TTF-1 promoter inhibited the growth of human lung cancer through the NDUFA4 pathway. Nucleic Acids 6, 183–197. https://doi.org/10.1016/j.omtn.2016.12.005.

Liang, Y., Zhao, Y., Li, L., Wei, H., Huang, T., Zhang, H., Chen, X., Yun, H., Sun, W., and Wang, Y. (2021). MicroRNA profiles in five pairs of early gastric cancer tissues and adjacent non-cancerous tissues. Oncol. Lett. 22, 595. https://doi.org/10.3892/ol.2021.12856.

London, W.B., Castel, V., Monclair, T., Ambros, P.F., Pearson, A.D., Cohn, S.L., Berthold, F., Nakagawara, A., Ladenstein, R.L., Iehara, T., and Matthay, K.K. (2011). Clinical and biologic features predictive of survival after relapse of neuroblastoma: a report from the International Neuroblastoma Risk Group project. J. Clin. Oncol. 29, 3286–3292. https://doi.org/10.1200/jco.2010.34.3392.

Maris, J.M., Hogarty, M.D., Bagatell, R., and Cohn, S.L. (2007). Neuroblastoma. Lancet 369, 2106–2120. https://doi.org/10.1016/S0140-6736(07)60983-0.

Maugeri, M., Barbagallo, D., Barbagallo, C., Banelli, B., Di Mauro, S., Purrello, F., Magro, G., Ragusa, M., Di Pietro, C., Romani, M., and Purrello, M. (2016). Altered expression of miRNAs and methylation of their promoters are correlated in neuroblastoma. Oncotarget 7, 83330–83341. https://doi.org/10.18632/oncotarget.13090.

Mohlin, S.A., Wigerup, C., and Påhlman, S. (2011). Neuroblastoma aggressiveness in relation to sympathetic neuronal differentiation stage. Semin. Cancer Biol. 21, 276–282. https://doi.org/10.1016/j.semcancer.2011.09.002.

Nakagawara, A., Arima, M., Azar, C.G., Scavarda, N.J., and Brodeur, G.M. (1992). Inverse relationship between trk expression and N-myc amplification in human neuroblastomas. Cancer Res. 52, 1364–1368.

Nakagawara, A., Azar, C.G., Scavarda, N.J., and Brodeur, G.M. (1994). Expression and function of TRK-B and BDNF in human neuroblastomas. Mol. Cell Biol. 14, 759–767. https://doi.org/10.1128/mcb.14.1.759.

Newman, E.A., and Nuchtern, J.G. (2016). Recent biologic and genetic advances in neuroblastoma: implications for diagnostic, risk stratification, and treatment strategies. Semin. Pediatr. Surg. 25, 257–264. https://doi.org/10.1053/j.sempedsurg.2016.09.007.

Ooi, C.Y., Carter, D.R., Liu, B., Mayoh, C., Beckers, A., Lalwani, A., Nagy, Z., De Brouwer, S., Decaesteker, B., Hung, T.T., et al. (2018). Network modeling of microRNA-mRNA interactions in neuroblastoma tumorigenesis identifies miR-204 as a direct inhibitor of MYCN. Cancer Res. 78, 3122–3134. https://doi.org/10.1158/0008-5472.CAN-17-3034.

Pacenta, H.L., and Macy, M.E. (2018). Entrectinib and other ALK/TRK inhibitors for the treatment of neuroblastoma. Drug Des. Develop. Ther. 12, 3549–3561. https://doi.org/10.2147/dddt.s147384.

Park, J.R., Bagatell, R., London, W.B., Maris, J.M., Cohn, S.L., Mattay, K.M., Hogarty, M., and Committee, C.O.G.N. (2013). Children's Oncology Group's 2013 blueprint for research: neuroblastoma. Pediatr. Blood Cancer 60, 985–993. https://doi.org/10.1002/pbc.24433.

Phelps, C.A., Lai, S.C., and Mu, D. (2018). Roles of thyroid transcription factor 1 in lung cancer biology. Vitamins Horm. 106, 517–544. https://doi.org/10.1016/bs.vh.2017.05.007.

Ryan, J., Tivnan, A., Fay, J., Bryan, K., Meehan, M., Creevey, L., Lynch, J., Bray, I.M., Bray, I.M., O'MeArA, A., et al. (2012). MicroRNA-204 increases sensitivity of neuroblastoma cells to cisplatin and is associated with a favourable clinical outcome. Br. J. Cancer 107, 967–976. https://doi.org/10.1038/bjc.2012.356.

Rydén, M., Sehgal, R., Dominici, C., Schilling, F.H., Ibáñez, C., and Kogner, P. (1996). Expression of mRNA for the neurotrophin receptor trkC in neuroblastomas with favourable tumour stage and good prognosis. Br. J. Cancer 74, 773–779. https://doi.org/10.1038/bjc.1996.435.

Saadi, I.J., Plyler, J.R., Bansal, H., Prajapati, S., Bansal, S., Rebeles, J., Chen, H.I.H., Chang, Y.F., Panneerdoss, S., Zoghi, B., et al. (2012). Genomic loss of tumor suppressor miRNA-204 promotes cancer cell migration and invasion by activating AKT/mTOR/Rac1 signaling and actin reorganization. PLoS One 7, e52397. https://doi.org/10.1371/journal.pone.0052397.

Samaraweera, L., Grandinetti, K.B., Huang, R., Spengler, B.A., and Ross, R.A. (2014). MicroRNAs define distinct human neuroblastoma cell phenotypes and regulate their differentiation and tumorigenicity. BMC Cancer 14, 309. https://doi.org/10.1186/1471-2407-14-309.

Shimada, H., Stram, D.O., Chatten, J., Joshi, V.V., Hachitanda, Y., Brodeur, G.M., Lukens, J.N., Matthay, K.K., and Seeger, R.C. (1995). Identification of subsets of neuroblastomas by combined histopathologic and N-myc analysis. J. Natl. Cancer Inst. 87, 1470–1476. https://doi.org/10.1093/jnci/87.19.1470.

Shimada, H., Umehara, S., Monobe, Y., Hachitanda, Y., Nakagawa, A., Goto, S., Gerbing, R.B., Stram, D.O., Lukens, J.N., and Matthay, K.K. (2001). International neuroblastoma pathology classification for prognostic evaluation of patients with peripheral neuroblastic tumors: a report from the Children's Cancer Group. Cancer 92, 2451–2461. https://doi.org/10.1002/1097-0142 (20011101)92:9<2451::aid-cncr1595>3.0.co;2-s.

Stallings, R.L. (2009). MicroRNA involvement in the pathogenesis of neuroblastoma: potential for microRNA mediated therapeutics. Curr. Pharm. Des. 15, 456–462. https://doi.org/10.2174/138161209787315837.

Stasevych, M., Zvarych, V., Lunin, V., Halenova, T., Savchuk, O., Dudchak, O., Vovk, M., and NoVikoV, V. (2015). Novel anthraquinone-based derivatives as potent inhibitors for receptor tyrosine kinases. Indian J. Pharm. Sci. 77, 634. https://doi.org/10.4103/0250-474x.169062.

Sticht, C., De La Torre, C., Parveen, A., and Gretz, N. (2018). miRWalk: an online resource for prediction of microRNA binding sites. PLoS One 13, e0206239. https://doi.org/10.1371/journal.pone.0206239.

Tan, Y.X., Hong, Y., Jiang, S., Lu, M.N., Li, S., Chen, B., Zhang, L., Hu, T., Mao, R., Mei, R., and Xiyang, Y.B. (2020). MicroRNA-449a regulates the progression of brain aging by targeting SCN2B in SAMP8 mice. Int. J. Mol. Med. 45, 1091–1102. https://doi.org/10.3892/ijmm.2020.4502.

Thomaz, A., Jaeger, M., Brunetto, A.L., Brunetto, A.T., Gregianin, L., de Farias, C.B., Ramaswamy, V., Nör, C., Taylor, M.D., and Roesler, R. (2020). Neurotrophin signaling in medulloblastoma. Cancers (Basel) 12, 2542. https://doi.org/10.3390/cancers12092542.

Thress, K., Macintyre, T., Wang, H., Whitston, D., Liu, Z.Y., Hoffmann, E., Wang, T., Brown, J.L., Webster, K., Omer, C., et al. (2009). Identification and preclinical characterization of AZ-23, a novel, selective, and orally bioavailable inhibitor of the Trk kinase pathway. Mol. Cancer Ther. 8, 1818–1827. https://doi.org/10.1158/1535-7163.MCT-09-0036.

Ueda, M., Iguchi, T., Nambara, S., Saito, T., Komatsu, H., Sakimura, S., Hirata, H., Uchi, R., Takano, Y., Shinden, Y., et al. (2015). Overexpression of transcription termination factor 1 is associated with a poor prognosis in patients with colorectal cancer. Ann. Surg. Oncol. 22, S1490–S1498. https://doi.org/10.1245/s10434-015-4652-7.

Wang, X., Qiu, W., Zhang, G., Xu, S., Gao, Q., and Yang, Z. (2015). MicroRNA-204 targets JAK2 in breast cancer and induces cell apoptosis through the STAT3/BCl-2/survivin pathway. Int. J. Clin. Exp. Pathol. 8, 5017–5025.

Winslow, M.M., Dayton, T.L., Verhaak, R.G.W., Kim-Kiselak, C., Snyder, E.L., Feldser, D.M., Hubbard, D.D., DuPage, M.J., Whittaker, C.A., Hoersch, S., et al. (2011). Suppression of lung adenocarcinoma progression by Nkx2-1. Nature 473, 101–104. https://doi.org/10.1038/nature09881.

Xiao, B., Lin, D., Zhang, X., Zhang, M., and Zhang, X. (2016). TTF1, in the form of nanoparticles, inhibits angiogenesis, cell migration and cell invasion in vitro and in vivo in human hepatoma through STAT3 regulation. Molecules 21, 1507. https://doi.org/10.3390/molecules21111507.

Yamaguchi, T., Hosono, Y., Yanagisawa, K., and Takahashi, T. (2013). NKX2-1/TTF-1: an enigmatic oncogene that functions as a double-edged sword for cancer cell survival and progression. Cancer Cell 23, 718–723. https://doi.org/10.1016/j.ccr.2013.04.002.

Yamashiro, D.J., Liu, X.G., Lee, C.P., Nakagawara, A., Ikegaki, N., McGregor, L.M., Baylin, S.B., Brodeur, G.M., and NAkAgAwArA, A. (1997). Expression and function of Trk-C in favourable human neuroblastomas. Eur. J. Cancer 33, 2054–2057. https://doi.org/10.1016/s0959-8049(97)00309-2.

Ying, Z., Li, Y., Wu, J., Zhu, X., Yang, Y., Tian, H., Li, W., Hu, B., Cheng, S.Y., and Li, M. (2013). Loss of miR-204 expression enhances glioma migration and stem cell-like phenotype. Cancer Res. 73, 990–999. https://doi.org/10.1158/0008-5472.CAN-12-2895.

Zhao, B.W., Jiang, S.S., Chen, Y.M., Huang, C.Y., and Li, Y.F. (2014). Reduced NKX2.1 expression predicts poor prognosis of gastric carcinoma. PLoS One 9, e114556. https://doi.org/10.1371/journal.pone.0114556.

STAR★METHODS

KEY RESOURCES TABLE

REAGENT or RESOURCE	SOURCE	IDENTIFIER
Antibodies		
Bcl-2	Abcam	ab182858
cleaved caspase-3	Abcam	ab32042
p53	Abcam	ab26
LC3B	Abcam	ab192890
p62	Abcam	ab109012
Beclin1	Abcam	ab210498
TTF1	Cell Signaling Technology	#12373
TrkA	Cell Signaling Technology	#2505
TrkB	Cell Signaling Technology	#4607
NSE	Abcam	ab180943
MAP2	Abcam	ab32454
TAU	Abcam	ab76128
GAPDH	Abcam	ab128915
Biological samples		
Tumour and tumour-adjacent tissues from patients with GN or NB	Guangzhou Women and Children's Medical Center	N/A
Chemicals, peptides, and recombinant proteins		
Trizol	Invitrogen	15596018
DMEM	Invitrogen	11965092
Lipofectamine 3000	Invitrogen	L3000001
Pepsin protease	Agilent Technologies	N/A
Propidium iodide	Sigma-Aldrich	P4864
Annexin V-FITC and PI	MultiSciences	70-APCC101-100
Matrigel	Corning	356234
Formaldehyde	Solarbio, China	P1110
Crystal violet	Solarbio	G1062
Glutaraldehyde	Aladdin, China	G105907
Osmium tetroxide	TED PELLA	18466
Uranyl acetate	Codow, China	CD106833
Ethanol	Sinopharm, China	100092683
Acetone	Sinopharm	10000418
Epoxy resin	Sinopharm	XW00000020
Ultramicrotome	Leica	RM2016
Methanol	Sinopharm	10014108
Bovine serum albumin	Solarbio	A8020
CCK-8 solution	Dojindo Molecular Technologies	CK04
EdU	RiboBio	C00003
RIPA lysis buffer	Beyotime	P0013C
Bicinchoninic acid assay	Thermo Fisher Scientific	23235
Chemiluminescence reagent	Millipore	11520709001

(Continued on next page)

Continued

REAGENT or RESOURCE	SOURCE	IDENTIFIER
Critical commercial assays		
Taqman miRNA Reverse Transcription Kit	Invitrogen	4366596
PrimeScriptTM RT Reagent Kit	Takara	RR047Q
RNA-LAPCR kit	Takara	N/A
SYBR Green qPCR Master Mix	DBI Bioscience	DBI-2043
Protein Immunoprecipitation Kit	Millipore	IP50
Deposited data		
RNA-seq data	This paper	GSE78061
Experimental models: Cell lines		
SK-N-BE	ATCC	CRL-2271
SK-N-SH	ATCC	HTB-11
SH-SY5Y	ATCC	CRL-2266
IMR-32	ATCC	CCL-127
293T	ATCC	CRL-3216
Experimental models: Organisms/strains		
Mouse: BALB/c nude mice (6-week-old, female)	Shanghai Laboratory Animal Center	N/A
Oligonucleotides		
Tables S3–S5	This paper	N/A
Software and algorithms		
SPSS 19.0	IBM	https://www.ibm.com/analytics/spss-statistics-software

RESOURCE AVAILABILITY

Lead contact

Further information and requests for resources and reagents should be directed to and will be fulfilled by the lead contact, Huimin Xia (xia-huimin@foxmail.com).

Materials availability

This study did not generate new unique reagents.

Data and code availability

- The RNA-seq data generated during this study are available at Gene Expression Omnibus (GEO): GSE78061.

- No original code was reported in this study.

- Any additional information required to reanalyze the data reported in this paper is available from the lead contact upon request.

EXPERIMENTAL MODEL AND SUBJECT DETAILS

Patients and samples

Tumour and tumour-adjacent tissues were collected from patients with GN, well-differentiated NB, and un-differentiated NB between 2014 and 2019 at Guangzhou Women and Children's Medical Center. All samples were immediately flash-frozen in liquid nitrogen and stored at −80°C. Specimens from patients with GN and NB were obtained prior to chemotherapy or radiotherapy. Clinical information was obtained from patients with GN and NB that underwent miRNA and RNA-seq (Table S1), and those used for external

verification (Table S2). This study was performed in accordance with the 1964 Helsinki declaration and approved by the ethical committee of Guangzhou Women and Children's Medical Center.

Cell lines

NB cell lines, including SK-N-BE (TrkA⁻TrkB⁺), SK-N-SH (TrkA⁺TrkB⁻), SH-SY5Y (TrkA⁻TrkB⁻), IMR-32 (TrkA⁺TrkB⁻), and 293T cells were purchased from the American Type Culture Collection (ATCC) and cultured in DMEM (Invitrogen, USA) containing 10% fetal bovine serum (FBS) and penicillin/streptomycin at 37°C with 5% CO_2.

Animal studies

Six-week-old female BALB/c nude mice (weighing 18–25 g) were purchased from the Shanghai Laboratory Animal Center (Shanghai, China) and housed in a specific pathogen free (SPF) environment with free access to food and water. Prior to inoculation, five groups of SK-N-BE cells were prepared: TTF1- or NC-transfected SK-N-BE cells, NC-transfected, NGF-treated, or NGF-treated+TTF1-transfected SK-N-BE cells. The cells were suspended in saline solution at a density of 2×10^6 cells/mL and injected subcutaneously into the right hind leg of the nude mice. Once xenograft tumours were visible to the naked eye, they were measured (length and width) and their volume calculated (formula: length×width²/2) 3, 7, 14, and 28 days after inoculation. After 28 days, all mice were sacrificed and the xenograft tumours were collected for subsequent analysis. All animal experiments were conducted in strict accordance with the Institutional Animal Protection and Use Committee of Guangzhou Women and Children's Medical Center.

METHOD DETAILS

RNA-seq and gene expression omnibus (GEO) database analysis

Total RNA was extracted from the flash-frozen tissue samples using Trizol reagent (Invitrogen, USA) and stored at −80°C. RNA quality was assessed using a NanoDrop ND-1000 (Thermo Fisher Scientific, USA). A cDNA library was constructed using RNA with an RNA integrity number (RIN) > 8.0 and RNA-seq was performed using an Illumina HiSeq 4000 (Illumina, San Diego, CA, USA). DE-Gs with a fold change >2 and a false discovery rate <0.05 were selected and significantly altered pathways were analysed using gene ontology (GO) analysis. A public GEO database of the NB cell line (GSE78061) was used to confirm TTF1, TrkA, and TrkB expression.

MiRNA sequencing (miRNA-seq)

MiRNA-seq was conducted by Aksomics (Shanghai, China) (Liang et al., 2021; Tan et al., 2020). Briefly, a library was constructed using the identified RNAs and its quality was confirmed using an Agilent 2100 Bioanalyzer. MiRNA-seq was then performed using an Illumina NextSeq 500 ® sequencing platform (Illumina). After the original reads had been screened using Solexa CHASTITY to obtain clean reads, known miRNAs were quantified and new miRNAs were predicted using miRDEEP2. Differentially expressed miRNAs (DEMs) were identified using R software.

Bioinformatics analysis

Target genes of the DEMs involved in NB were predicted using the miRDB, TargetScan, and miRTarBase prediction tools in miRWalk (http://mirwalk.umm.uni-heidelberg.de/) (Sticht et al., 2018). The function of the DEMs was analysed using GO, including molecular functions (MFs), biological processes (BPs), and cellular components (CCs). MiRNA target genes were also subjected to Kyoto Encyclopedia of Genes and Genomes (KEGG) pathway enrichment analysis using DAVID 6.8 (Da et al., 2008). Log10 (p value) enrichment scores indicated statistical significance with an adjusted p value of <0.01.

Cell transfection

NB cell lines, including SK-N-BE (TrkA⁻TrkB⁺), SK-N-SH (TrkA⁺TrkB⁻), SH-SY5Y (TrkA⁻TrkB⁻), IMR-32 (TrkA⁺TrkB⁻), and 293T cells were purchased from the American Type Culture Collection (ATCC) and cultured in DMEM (Invitrogen, USA) containing 10% fetal bovine serum (FBS) and penicillin/streptomycin at 37°C with 5% CO_2. Cells were transfected for 48 h using Lipofectamine 3000 (Invitrogen) with si-negative control (NC), TTF1-siRNA (si-TTF1), and TrkA-siRNA (si-TrkA) purchased from GenePharma (Suzhou, China). Human TTF1 full-length cDNAs were amplified from mRNAs using RT-PCR with specific primers. Human TrkB full-length cDNAs were amplified using RT-PCR with specific primers. Primer sequences are listed in Table S3. The PCR products were then inserted into a pcDNA 3.1 vector and confirmed using

sequencing as TTF1- and TrkB- overexpression plasmids, respectively. Briefly, SK-N-BE and SH-SY5Y cells were transfected with the TTF1-overexpression plasmid and negative control (NC), while SK-N-SH and IMR-32 cells were transfected with TTF1-siRNA (si-TTF1) and si-NC. For the rescue experiments, TTF1-over-expressing SK-N-BE cells were transfected with a miR-204 inhibitor, while SK-N-BE cells were co-trans-fected with the TTF1-overexpression plasmid and si-TrkA or TrkB-overexpression plasmid, respectively. For the induced-differentiation experiments, SK-N-BE cells were pre-treated with 100 ng/mL NGF for 30 min and then transfected with the TTF1-overexpression plasmid.

RT-qPCR

Extracted RNA samples were reversed-transcribed into cDNA using a Taqman miRNA Reverse Transcrip-tion Kit (Invitrogen) or a PrimeScript^{TM} RT Reagent Kit (Takara, Tokyo, Japan) according to the manufac-turer's protocol. PCR was performed using 500 ng of DNase-treated total RNA and an RNA-LAPCR kit (Takara) for TTF1, TrkA, TrkB, NSE, MAP2, and TAU, with SYBR Green qPCR Master Mix (DBI Bioscience, Germany) for the specific miRNAs. The relative expression of the selected genes was calculated using the comparative cycle threshold (CT) $2^{-\Delta\Delta Ct}$ method. Primer sequences are listed in Table S4. U6 or GAPDH were used as internal controls.

Fluorescence *in situ* hybridization (FISH)

MiR-204 expression was detected in GN, well-differentiated NB, and undifferentiated NB tissues (de Pla-nell-Saguer et al., 2010). Briefly, a locked nucleic acid-conjugated miR-204-specific probe against the mature miR-204 sequence was synthesized by Exiqon (Qiagen GmbH, Germany). Tissue samples were embedded in paraffin, cut into 6 μm sections, deparaffinized, and treated with Pepsin protease (Agilent Technologies, USA) for 30 min at 37°C. After hybridization with miR-204-specific probes followed by anti-digoxigenin HRP-conjugated antibodies, nuclei were stained with 4′,6-diamidino-2-phenylindole (DAPI) and hybridization signals were detected using a Nikon ECLIPSE Ti confocal microscope.

Luciferase reporter assay

According to the binding sequences between TTF1 and the TrkA promoter or miR-204 predicted using the ENCODE H3K4Me3 region, wild type and mutant sequences of the TrkA promoter or miR-204 were in-serted into the pGL3-Basic Vector. 293T cells were co-transfected with the TTF1 overexpression plasmid together with pGL3-WT-TrkA or pGL3-MUT-TrkA, as well as pGL3-WT-miR-204 or pGL3-MUT-miR-204. Data were presented as the ratio of Firefly to Renilla luciferase activity. Based on the putative binding sites between miR-204 and 3′UTR of human TrkB, psiCheck2 vectors containing the wild-type and mutant-type reporter 3′UTR of TrkB (TrkB-WT and TrkB-MUT) were synthesized by GenePhama (China). 293T cells were co-transfected with TrkB-WT and miR-204 mimics or NC, TrkB-MUT, and miR-204 mimics or NC. Data were presented as the ratio of Renilla to Firefly luciferase activity. All transfection protocols were performed for 48 h and relative luciferase activity was measured using a dual luciferase assay kit (Promega, USA).

RNA immunoprecipitation (RIP) assay

RIP assays were performed using a Protein Immunoprecipitation Kit (Millipore, USA). Briefly, NB cells were transfected with NC or miR-204 mimics, lysed with RIP lysis buffer, and incubated with RIP buffer containing magnetic beads conjugated with anti-Ago2 antibodies (Active Motif, #25500) or normal IgG (Millipore). Co-precipitated RNA (TrkB) levels were detected using RT-qPCR.

DNA bisulphite treatment and methylation-specific PCR (MSP)

Genomic DNA from tissues or tumour cells was treated using an EpiTect bisulphite kit (Qiagen; •, methyl-ated CpG cytosine; ○, unmethylated CpG cytosine). Gene methylation was determined using AmpliTaq Gold and MSP. CpG sites and MSP primers (Table S5) were determined using MethPrimer, as reported pre-viously (Kondo et al., 2009).

Flow cytometry analysis

Transfected cells were harvested, washed twice with phosphate-buffered saline (PBS), and treated with 0.25% EDTA-trypsin for 4 h at 37°C. For the cell cycle assay, adherent cells were suspended in PBS and stained with 50 μg/mL propidium iodide (PI, Sigma-Aldrich, USA) for 30 min. Cells in G0/G1, S, and G2/M phases were quantified using flow cytometry (BD Biosciences, USA). To detect apoptosis, cells were fixed

with ice-cold 70% ethanol for 2 h at 4°C, stained with Annexin V-FITC and PI (70-APCC101-100, MultiSciences, China), and quantified using flow cytometry (BD Biosciences) with Modfit software.

Wound healing assay

Transfected cells were seeded into 24-well plates (1 × 10^6/well) and incubated at 37°C. A wound was created in the cell monolayer using a 100 μL pipette tip and the cells were cultured in serum-free medium for 48 h. Images of the experimental and control groups were captured at 0 and 48 h, respectively, and the relative wound area was calculated.

Cell invasion assay

Approximately 5 × 10^5 transfected cells in serum-free media were added to the upper chamber of Transwell inserts (3422, Costor, China) coated with diluted Matrigel (0.3 mg/mL; 356234, Corning, China). The lower chamber was filled with media containing 20% FBS as a chemoattractant. After incubation for 24 h, cells that had migrated into the lower chamber were fixed with 4% formaldehyde (P1110, Solarbio, China) for 15 min, stained with 0.2% crystal violet (G1062, Solarbio) at room temperature, and counted in five random fields under a microscope (magnification, 20×).

Transmission electron microscopy (TEM)

Transfected cells were fixed with 2.5% glutaraldehyde (G105907, Aladdin, China) at 4°C overnight, followed by 2% osmium tetroxide (18466, TED PELLA, USA). After the cells had been stained with 1% uranyl acetate (CD106833, Codow, China), they were dehydrated with a gradient concentration of ethanol (100092683, Sinopharm, China) and acetone (10000418, Sinopharm), embedded in epoxy resin (XW00000020, Sinopharm), and sectioned using an ultramicrotome (RM2016, Leica, China). Autophagosomes were observed using TEM (Hitachi, Tokyo, Japan).

Immunofluorescence (IF) assay

Cells from different groups were fixed with 4% formaldehyde, washed with PBS, and permeabilized using 100% methanol (10014108, Sinopharm) at −20°C. The cells were then blocked with 1% bovine serum albumin (BSA, A8020, Solarbio) and incubated with primary antibodies against TTF1, TrkA, TrkB, NSE, MAP2, and TAU overnight at 4°C. After the samples had been rinsed three times in PBS containing 0.1% Tween 20, they were incubated with appropriate secondary antibodies for 2 h at room temperature. Cell nuclei were stained with DAPI and fluorescent images were captured using a FV10i confocal microscope (Olympus, Japan).

CCK-8 assay

Transfected SK-N-SH, SK-N-BE, and SH-SY5Y cells were seeded into 96-well plates at a density of 3 × 10^3 cells/well. After 24, 48, and 72 h, respectively, the cells were incubated with CCK-8 solution (20 μL/well; Dojindo Molecular Technologies, USA) at 37°C for 2 h and the optical density of each well was measured at 450 nm using a microplate reader (Multiscan MK3, Thermo Fisher, China).

Colony formation assay

Transfected cells were seeded into 12-well plates at a density of 2,500 cells/well and grown for seven consecutive days to form clearly visualized colonies. The cells were then washed with PBS, fixed with 4% paraformaldehyde for 15 min, washed with PBS, and stained with 0.2% crystal violet for 10 min. After being rinsed again with PBS, the colonies were air-dried, photographed, and counted under a light microscope.

EdU assay

Transfected cells were washed with PBS, incubated in serum-free DMEM for 2 h with EdU (10 μmol/L, RiboBio, Guangzhou, China), and stained with Apollo and DAPI. The stained cells were imaged using fluorescence microscopy (Olympus) and the ratio of EdU positive cells was calculated.

Western blot analysis

Total protein was extracted from cells in different groups after lysis with RIPA lysis buffer (Beyotime). Protein concentration was determined using a bicinchoninic acid assay (Thermo Fisher Scientific, USA). Equal amounts of protein samples were subjected to SDS-polyacrylamide gel electrophoresis and transferred

onto PVDF membranes that were blocked with 5% milk powder containing 0.1% TBS-Tween-20, and incubated with specific primary antibodies against Bcl-2 (ab182858; Abcam, USA), cleaved caspase-3 (ab32042; Abcam), p53 (ab26; Abcam), LC3B (ab192890; Abcam), p62 (ab109012; Abcam), Beclin1 (ab210498; Abcam), TTF1 (#12373; CST, USA), TrkA (#2505; CST), TrkB (#4607; CST), NSE (ab180943; Abcam), MAP2 (ab32454; Abcam), TAU (ab76128; Abcam), and GAPDH (ab128915; Abcam) at 4°C overnight. After incubation with HRP-linked secondary antibodies (BA1051 and BA1054; BOSTER, China) for 2 h at room temperature, protein bands were visualized using chemiluminescence reagent (Millipore, USA) in a Bio-Rad Universal Hood II DOC Electrophoresis Imaging Cabinet.

Immunohistochemistry (IHC)

Xenograft tumours were fixed in 10% buffered formalin, embedded in paraffin, and cut into 4 μm sections that were deparaffinized and rehydrated in a graded alcohol series. Following antigen retrieval, the slides were incubated overnight at 4°C with primary antibodies against TTF1, TrkA, TrkB, LC3B, p62, p53, MAP2, NSE, and TAU, followed by peroxidase-conjugated secondary antibodies for 2 h at room temperature. An EnVision Detection System kit (DAKO, Denmark) was used to detect the DAB chromogen followed by nuclear staining using haematoxylin.

QUANTIFICATION AND STATISTICAL ANALYSIS

All experiments were conducted at least three times and statistical analysis was performed using SPSS 19.0 software (SPSS). Data were expressed as the mean ± standard deviation (SD). Differences between groups were calculated using unpaired Student's t-tests or one-way ANOVA followed by Tukey's post-hoc multiple comparison tests. p values of <0.05 were considered statistically significant.